von Blanckenburg, F., Bouchez, J., Wittmann, H. (2012): Earth surface erosion and weathering from the 10Be (meteoric)/9Be ratio. - Earth and Planetary Science Letters, 351, 352, 295-305

DOI: 10.1016/j.epsl.2012.07.022

Earth surface erosion and weathering from the ^{10}Be (meteoric)/^{9}Be ratio

Friedhelm von Blanckenburg*, Julien Bouchez, and Hella Wittmann

GFZ German Research Centre for Geosciences, Telegrafenberg, 14473 Potsdam, Germany

* corresponding author: fvb@gfz-potsdam.de, tel: +49-331-2882850, fax +49-331-2882852

Earth and Planetary Science Letters v351-352, pp 295-305 2012, doi j/epsl.2012.07.022

Abstract

The isotope ratio of the meteoric cosmogenic nuclide ^{10}Be to the mineral-derived stable isotope ^{9}Be discloses both the Earth surfaces' denudation rate and its weathering intensity. We develop a set of steady state mass balance equations that describes this system from a soil column over the hillslope scale to an entire river basin. The prerequisites making this new approach possible are: 1) the ^{9}Be concentration of parent rock (typically 2.5 ± 0.5 ppm in granitic and clastic sedimentary lithologies) is known; 2) both Be isotopes equilibrate between the fluids decomposing rock and reactive solids formed during weathering; and 3) a critical spatial scale is exceeded at which the fluxes of both isotopes into and out of the weathering zone are at steady state over the time scale of weathering (typically ~10 kyr). For these cases the isotope ratios can be determined in bulk sediment or soil, on leachates from the reactive (adsorbed and pedogenic mineral-bound) phase in sediment or soil, and even on the dissolved phase in river water. The ^{10}Be/^{9}Be ratio offers substantial advantages over the single-isotope system of meteoric ^{10}Be. The latter system allows to directly determine erosion rates only in the case that ^{10}Be is fully retentive in the weathering zone and that riverine sorting has not introduced grain size-dependent ^{10}Be concentration gradients in sediments. We show the feasibility of the ^{10}Be/^{9}Be tracer approach at the river scale for sediment and water samples in the Amazon basin, where independent estimates of denudation rates from *in situ*-produced ^{10}Be exist. We furthermore calculate meaningful denudation rates from a set of published ^{10}Be/^{9}Be ratios measured in the dissolved load of globally distributed rivers. We conclude that this isotope ratio can be used to reconstruct global paleo-denudation from sedimentary records.

Keywords: Earth surface processes, cosmogenic nuclides, critical zone, river weathering and erosion fluxes, Amazon river

Introduction

The ratio of the meteoric cosmogenic fallout nuclide ^{10}Be ($T_{1/2}$ = 1.39 My) to the stable isotope ^{9}Be is a most promising weathering proxy. The system combines a tracer of known flux to the Earth surface with one that depends on its release rate from rock by weathering. Consequently it was suggested that this isotope ratio depends on global denudation when measured in seawater (Bourlès et al., 1989; Brown et al., 1992b; von Blanckenburg et al., 1996). Moreover, it was proposed that this isotope ratio records denudation back through time when extracted from authigenic ocean sedimentary records (Bourlès et al., 1989; von Blanckenburg and O'Nions, 1999). Following from these observations, Willenbring and von Blanckenburg (2010a) have used the ^{10}Be/^{9}Be isotope ratio in ocean deposits over the past 10 My to infer that the global denudation rate was constant over this period. Despite holding so much promise, this system was explored in detail in only two pioneering studies: Brown et al. (1992a) explored the ^{10}Be/^{9}Be ratio in dissolved and suspended loads of the Orinoco and the Amazon river basins, and Barg et al. (1997) used the ratio in the authigenic phase of soils, to infer soil ages and assess open system behaviour of soils. The mechanisms that set this isotope ratio in the compartments of the Earth surface, however, remain to date still widely unexplored.

Improving our understanding of ^{10}Be/^{9}Be ratio system is timely since the single-isotope system meteoric ^{10}Be is currently receiving much renewed interest as a tracer for terrestrial Earth surface stability. This method, explored first by Lal and Peters (1967), was established as a monitor of basin-wide erosion in two pioneering studies of river sediment by L. Brown et al. (1988) and You et al. (1988), but was partially sidelined in the years that followed by the astounding success of the "sister nuclide", *in situ*-produced ^{10}Be measured in quartz to determine exposure ages and rates of denudation (Lal, 1991). The advantages of the meteoric variety of ^{10}Be over the *in situ*-produced nuclide lie in this isotopes' higher concentrations, requiring smaller sample amounts, its applicability to quartz-free lithologies, and the possibility to determine denudation rate time series in fine-grained sedimentary deposits. Recent improvements in our understanding of the spatial and temporal patterns of delivery of the meteoric fallout nuclide (summarised in Willenbring and von Blanckenburg (2010b)) and overviews of its distribution in soils (Graly et al., 2010) are currently triggering new applications in erosional settings (e.g. Jungers et al., 2009).

However, quantitative estimates of erosion using the meteoric ^{10}Be tracer are compromised by the highly variable retention behavior of Be in soils and river sediment. Be is firmly adsorbed onto particles only if the coexisting solution pH exceeds a value of 6 (You et al., 1989; Aldahan et al., 1999; Willenbring and von Blanckenburg, 2010b). Furthermore, once soil particles have been transferred into streams, they will be sorted by grain size, which adds further complexity as the extent of Be adsorption onto solids is highly grain size-dependent (Willenbring and von Blanckenburg, 2010b).

Both retentivity and grain size issues can be circumvented when ^{10}Be concentration is normalised over a second element that has similar partitioning behavior between solid and solution. The optimal normalizing counterpart is, of course, another isotope of the same element, since its chemical properties are identical. The isotope ^{9}Be, the stable counterpart of ^{10}Be, is present in concentrations of a few ppm in most rocks, and is potentially ideal to serve for this purpose, provided we understand the way this stable isotope is released during weathering, mixed with meteoric ^{10}Be, and partitioned between particles and solution. Realising this stable isotopes' potential, Bacon et al. (2012) have recently employed ^{9}Be concentrations to quantify the loss of ^{10}Be from a soil profile.

The aim of this study is to provide a quantitative framework that allows to interpret ^{10}Be/^{9}Be ratios as a proxy of denudation rates in bulk soil and in river sediment in their "reactive" phase (*i.e.* adsorbed onto mineral surfaces and precipitated in secondary weathering products), and in solution. Many of the issues and assumptions involving the meteoric single-isotope ^{10}Be tracer were discussed extensively by Willenbring and von Blanckenburg (2010b). Here we first present a simple steady state mass balance for Be isotopes in the

weathering zone, and discuss the assumptions that are made to establish this mass balance. We demonstrate the feasibility of this approach by applying it to the tributaries and trunk stream of the Amazon River, for which an exceptional wealth of hydrologic data, meteoric ^{10}Be concentrations, ^{10}Be/^{9}Be ratios, and denudation rates from *in situ*-produced cosmogenic nuclides exist. We finally apply the concept to ^{10}Be/^{9}Be ratios measured in the dissolved and the reactive phase to published data on large rivers. Altogether, we show that both denudation rate and the degree of weathering of an entire river basin can be derived by measuring ^{10}Be/^{9}Be ratios in weathering products.

2. A conceptual framework for the ^{10}Be/^{9}Be system at the Earth's surface

We develop a steady state mass balance for both ^{9}Be and ^{10}Be, for which one principal assumption is made that is later explored in detail: over a certain time scale the two isotopes leave the weathering zone at the same rate as they enter the zone (Fig. 1). This time scale can be broadly defined as four to five times the residence time of Be in the weathering zone. For ^{10}Be, the residence time is the ratio of the inventory of ^{10}Be in a vertical soil column divided by the atmospheric flux of ^{10}Be. For ^{9}Be, the residence time is similar to the denudation time scale (the ratio of the depth of the weathering zone divided by the denudation rate D, in kg m^{-2} yr^{-1}). Both residence times are typically in the range of 10^3-10^5 yr. ^{10}Be/^{9}Be ratios result for the different Be compartments exported out of the zone: a) Be contained in bulk solid (typically river sediment), b) solid secondary weathering products containing Be, and c) Be dissolved in water.

2.1 ^{10}Be and ^{9}Be mass balance during steady-state weathering

The sole source of meteoric ^{10}Be to the weathering zone is atmospheric fallout, through both wet or dry deposition (Monaghan et al., 1985/86; Field et al., 2006; Heikkilä et al., 2008) (Fig. 1). Production of *in situ* ^{10}Be is regarded as negligible compared to the flux of meteoric ^{10}Be (Willenbring and von Blanckenburg, 2010b). A certain fraction of ^{10}Be atoms delivered to the Earth's surface adsorbs onto mineral surfaces or co-precipitates with Fe- and Al-oxides or hydroxides, with amorphous alumino-silicates, with clays, or with carbonates. This ^{10}Be pool exchanges with dissolved ^{10}Be through dissolution- precipitation or desorption-adsorption reactions and is thus called "reactive" (^{10}Be$_{reac}$). The remaining ^{10}Be atoms are exported as dissolved compounds (^{10}Be$_{diss}$). We further assume that the residence time of ^{10}Be in the system is short compared to its radioactive half-life (1.39 My, Chmeleff et al., 2010; Korschinek et al., 2010). This assumption is evaluated in detail by Willenbring and von Blanckenburg (2010b) and was found valid for most eroding settings.

At steady-state, the fluxes of ^{10}Be are balanced:

$$F_{met}^{^{10}Be} = E * \left[^{10}Be\right]_{reac} + Q * \left[^{10}Be\right]_{diss} \quad (1)$$

where $F_{met}^{^{10}Be}$ is the flux of meteoric ^{10}Be to the Earth's surface (in atoms m^{-2} yr^{-1}), E is the erosion flux (in kg m^{-2} yr^{-1}), Q is the water flux out of the system (in m^3 m^{-2} yr^{-1} or equivalently in m yr^{-1}), and $[^{10}Be]_{reac}$ and $[^{10}Be]_{diss}$ represent the concentrations of reactive and dissolved ^{10}Be (respectively in atoms kg^{-1} and atoms L^{-1}).

In most geomorphic field experiments, $[^{10}Be]_{diss}$ is not available. We make use of the Be partition coefficient K_d (in L kg^{-1}) that links Be concentrations in the reactive and dissolved phases:

$$K_d = \frac{[Be]_{reac}}{[Be]_{diss}} \quad (2)$$

In our model weathering system K_d can be used because the reactive phase and water are assumed to be at chemical equilibrium via continuous exchange of Be. K_d depends on the nature of the solid, temperature,

chemical composition of the solution (pH, competing ions, presence of organic matter) but not on the solid/fluid ratio. For Be, K_d is highly pH-dependent: its value is 10^3 L kg^{-1} for pH between 4 and 5, 10^4 L kg^{-1} at pH between 5 and 6 and 10^5 L kg^{-1} at pH above 6 (You et al., 1989; Aldahan et al., 1999). Substituting eq. (2) into eq. (1) yields:

$$E = \frac{{}^{10}F_{met}^{Be}}{[{}^{10}Be]_{reac}} - \frac{Q}{K_d} \quad (3)$$

Eq. (3) allows to calculate erosion rates E from a measurement of $[{}^{10}Be]_{reac}$. Accurate erosion rates can only be determined if Q and K_d are known over the residence time of Be in the weathering zone. However, we can simplify this condition in settings where $Q/K_d << E$, meaning either that the water flux Q is low, or that the erosion rate E is high, or that Be has a high affinity for the reactive phase such that K_d is high. Then:

$$E = \frac{{}^{10}F_{met}^{Be}}{[{}^{10}Be]_{reac}} \quad (4)$$

which corresponds to eq. (21) in Willenbring and von Blanckenburg (2010b) or the equation generally used for erosion studies of the single-isotope meteoric ^{10}Be system (Brown et al., 1988). An assessment of the bias introduced by this simplification is presented in Appendix A.1.

The ^{9}Be system can be defined as follows. Bedrock, containing ^{9}Be in its minerals (^{9}Be$_{parent}$), continuously enters the weathering zone through the advance of the weathering front (Fig. 1). Chemical weathering results in the partial dissolution of bedrock and leads to a release of ^{9}Be. The dissolution of ^{9}Be from bedrock is not necessarily congruent, and a fraction termed ^{9}Be$_{min}$ remains locked in primary minerals. The released ^{9}Be that adsorbs onto mineral surfaces or is incorporated into precipitates is called ^{9}Be$_{reac}$. The ^{9}Be remaining in solution, called ^{9}Be$_{diss}$, is exported as dissolved material into water. At steady-state, the fluxes of ^{9}Be are balanced:

$$D * [{}^{9}Be]_{parent} = E * \left([{}^{9}Be]_{min} + [{}^{9}Be]_{reac}\right) + Q * [{}^{9}Be]_{diss} \quad (5)$$

where $[{}^9Be]$ are ^{9}Be concentrations, in atoms kg^{-1} or mol kg^{-1}. Note that only the ^{9}Be that is released from primary minerals by chemical weathering mixes with ^{10}Be. We can single out this component by recasting this mass balance in terms of non-dimensional ^{9}Be fractional fluxes ($f^{{}^{9}Be}$), calculated by dividing eq. (5) by $D * [{}^9Be]_{parent}$:

$$1 = f_{min}^{{}^{9}Be} + f_{reac}^{{}^{9}Be} + f_{diss}^{{}^{9}Be} \quad (6)$$

where the term $f_{reac}^{{}^{9}Be} + f_{diss}^{{}^{9}Be}$ represents the fraction of ^{9}Be that is released from primary minerals. This fraction is a measure for the degree of weathering. Assuming that the effects of isotope fractionation between dissolved and reactive Be are much smaller than the range in ^{10}Be/^{9}Be ratios set during weathering, we can use the same K_d for Be, ^{9}Be or ^{10}Be. Using the definition of K_d (eq. 2) for ^{9}Be, and rearranging eq. (5) yields the following intermediate expression:

$$[{}^{9}Be]_{reac} = \frac{D*[{}^{9}Be]_{parent} - E*[{}^{9}Be]_{min}}{E + \frac{Q}{K_d}} \quad (7)$$

When combining the mass balance approaches for ^{9}Be and ^{10}Be, respectively, by solving eq. 3 for $[{}^{10}Be]_{reac}$ and combining it with the expression of $[{}^9Be]_{reac}$ given in eq. (7), we obtain a ratio $({}^{10}Be/{}^{9}Be)_{reac}$. At

equilibrium this ratio is identical to $(^{10}Be/^{9}Be)_{diss}$, ignoring a minor mass-dependent isotope fractionation. Hence :

$$\left(\frac{^{10}Be}{^{9}Be}\right)_{reac} = \left(\frac{^{10}Be}{^{9}Be}\right)_{diss} = \frac{^{10}F_{met}}{D*[\,^{9}Be]_{parent} - E*[\,^{9}Be]_{min}} \quad . \tag{8}$$

Equation (8) explicitly shows that the ratio between ^{10}Be and ^{9}Be (present in the dissolved or in the reactive phase) is the ratio between the flux of ^{10}Be delivered to the Earth surface and the flux of ^{9}Be released by weathering (i.e. the ^{9}Be passing through the weathering front minus the amount that remains locked in primary minerals). In other words, using ^{9}Be flux fractions (eq. 6):

$$\left(\frac{^{10}Be}{^{9}Be}\right)_{reac} = \left(\frac{^{10}Be}{^{9}Be}\right)_{diss} = \frac{^{10}F_{met}}{D*[\,^{9}Be]_{parent}*\left(f_{reac}^{\,^{9}Be} + f_{diss}^{\,^{9}Be}\right)} \quad . \tag{9}$$

Importantly, in eqs. (8) and (9), the ratios $(^{10}Be/^{9}Be)_{reac}$ and $(^{10}Be/^{9}Be)_{diss}$ are independent of whether this ^{9}Be was portioned into the reactive or into the dissolved phase. They rather depend on the term $f_{reac}^{\,^{9}Be} + f_{diss}^{\,^{9}Be}$, which describes the amount of ^{9}Be that was dissolved from primary minerals. This behavior differs in an important way from that of the single isotope system $^{10}Be_{reac}$ (eq. 3), in which, for a given erosion rate, the concentration depends linearly on the loss of ^{10}Be into solution.

The functional relationship described by eq. (9) is shown in Fig. 2. An increase in denudation rate at constant $f_{reac}^{\,^{9}Be} + f_{diss}^{\,^{9}Be}$, and hence constant degree of weathering, follows the oblique line downward. An increase in the degree of weathering whilst keeping *D* constant results in a lowering of $(^{10}Be/^{9}Be)_{reac}$ or $(^{10}Be/^{9}Be)_{diss}$.

D can be read from this diagram for a measured ^{10}Be/^{9}Be ratio if $f_{reac}^{\,^{9}Be} + f_{diss}^{\,^{9}Be}$ is known. A test of the model is possible if we assume that a reasonable lower limit for the fraction of ^{9}Be released from primary minerals is 0.1 (section 3), and denudation rates are available for a given setting from independent means. In that case all data shall plot within this array. This approach is carried out for the Amazon basin in section 4. If such independent information is not available, eqs. (8) and (9) can be difficult to use in practice as the isotope ratios depend on two unknowns : *D*, and *E* or weathering intensity in the form of $f_{reac}^{\,^{9}Be} + f_{diss}^{\,^{9}Be}$. Solving eq. (5) for *E* and substituting into eq. (8) yields (intermediate steps are presented in online supplement S.1):

$$\left(\frac{^{10}Be}{^{9}Be}\right)_{reac} = \left(\frac{^{10}Be}{^{9}Be}\right)_{diss} = \frac{\frac{^{10}F_{met}}{D*[\,^{9}Be]_{parent}}\left(\frac{[\,^{9}Be]_{min}}{[\,^{9}Be]_{reac}} + 1\right)}{1 + \frac{Q}{K_d} * \frac{[\,^{9}Be]_{min}}{D*[\,^{9}Be]_{parent}}} \tag{10}$$

A denudation rate can also be calculated from total Be in bulk sediment. For this case $(^{10}Be/^{9}Be)_{total}$ is defined as the ^{10}Be/^{9}Be ratio in the bulk solid material exported from the weathering system. Since $[^{9}Be]_{total} = [^{9}Be]_{reac} + [^{9}Be]_{min}$ and $[^{10}Be]_{total} = [^{10}Be]_{reac}$:

$$\left(\frac{^{10}Be}{^{9}Be}\right)_{total} = \frac{\frac{^{10}F_{met}}{D*[\,^{9}Be]_{parent}}}{1 + \frac{Q}{K_d} * \frac{[\,^{9}Be]_{min}}{D*[\,^{9}Be]_{parent}}} \tag{11}$$

The advantage of eqs. (10) and (11) is that they contain measurable quantities only. However, these equations contain a Q/K_d term, which seems to indicate that $(^{10}Be/^{9}Be)_{reac}$ or $(^{10}Be/^{9}Be)_{diss}$ depend on Be

retention and water flux. This dependence is only apparent (online supplement S.2). Yet while the ratios $(^{10}Be/^{9}Be)_{reac}$ or $(^{10}Be/^{9}Be)_{diss}$ are not dependent on discharge or on retentivity, using eqs. (10) and (11) to calculate D in practice still requires knowing Q/K_d. Similar to the single isotope system (eq. 3), eqs. (10) and (11) can be simplified if $Q/D << K_d*[^{9}Be]_{parent}/[^{9}Be]_{min}$, leading to:

$$\left(\frac{^{10}Be}{^{9}Be}\right)_{reac} = \left(\frac{^{10}Be}{^{9}Be}\right)_{diss} = \frac{^{10}F_{met}^{Be}}{D*[^{9}Be]_{parent}}\left(\frac{[^{9}Be]_{min}}{[^{9}Be]_{reac}} + 1\right) \quad (12)$$

$$\left(\frac{^{10}Be}{^{9}Be}\right)_{total} = \frac{^{10}F_{met}^{Be}}{D*[^{9}Be]_{parent}} \quad (13)$$

An assessment of the bias in denudation rate resulting from using the simplified eqs. (12) and (13) is shown in Appendix A.2. Importantly, the bias is smaller the higher the degree of weathering.

Denudation rates can be determined from eq. (12) or eq. (13) using $^{10}Be/^{9}Be$ ratios measured in river sediment, for example. Note that $(^{10}Be/^{9}Be)_{reac}$ measured in river sediment does not depend on grain size (section 4). In contrast, measured $(^{10}Be/^{9}Be)_{total}$ (eq. 13) might be grain size-dependent, since fine grains will yield a higher $[^{9}Be]_{reac}$ and hence $[^{9}Be]_{total}$ than coarse grains. Solving eq. (10) or (12) requires knowing $[^{9}Be]_{min}/[^{9}Be]_{reac}$. This ratio likely depends on grain size for the same reasons as does $(^{10}Be/^{9}Be)_{total}$. However, in settings where the degree of weathering is high, $[^{9}Be]_{min}/[^{9}Be]_{reac}$ is close to 0 (since most Be has been unlocked from primary minerals) and then $(^{10}Be/^{9}Be)_{reac}$ is nearly equal to $(^{10}Be/^{9}Be)_{total}$. In this case, both the ratios are independent of grain size when measured in river sediment. Hence in such settings D can be determined from a measurement of a $^{10}Be/^{9}Be$ ratio in three different ways: measured either in (1) a bulk river sediment, bedload or suspended load (eq. 13); (2) in the reactive phase of this river sediment (eq. 12); or (3) on a sample of filtered river water (eq. 12).

3. Assumptions and requirements

Next we discuss a series of assumptions that are made in the mass balance presented above and the requirements that have to be met for determining E and D from $^{10}Be/^{9}Be$ ratios measured on field samples.

The meteoric flux of ^{10}Be is known. Knowing this flux accurately is the most important prerequisite of both the single-isotope ^{10}Be method as of the $^{10}Be/^{9}Be$ ratio approach (Monaghan et al., 1985/86). However, it is well-known that $^{10}F_{met}^{Be}$ varies both spatially and temporarily (Vonmoos et al., 2006). These variations have been reviewed in detail by Willenbring and von Blanckenburg (2010b). On the large drainage basin scale, the distribution of $^{10}F_{met}^{Be}$ can be read from fallout maps produced by combined cosmogenic nuclide production and atmospheric general circulation models (Field et al., 2006; Heikkilä et al., 2008) and varies from 0.4 to 1.5 x 10^6 atoms cm^{-2} yr^{-1}. Over the small spatial scale, this flux potentially depends on short-scale orographic effects and other differences in precipitation, depending whether the additive or the dilution effect controls the concentration of ^{10}Be in rain (Willenbring and von Blanckenburg, 2010b).

$[^{9}Be]_{parent}$ is known. Very conveniently, most crustal rocks feature an average Be concentration of 2.5 ppm (Table 1, Fig. 3) as compiled in global geochemical data sets (Staudigel et al., 1998; Grew, 2002). The average Be concentration of the upper continental crust was estimated at 2.2 ± 0.5 ppm (Rudnick and Gao, 2004). Hence, a mean $[^{9}Be]_{parent}$ can be used in large basin studies, and the systematic bias introduced by this assumption does not exceed very much that stemming from all other assumptions. For all calculations in this text we use $[^{9}Be]_{parent}$ of 2.5 ppm. However, the validity of this assumption strongly depends on the spatial scale of the investigation. This assumption is valid on the scale of a large river basin such as that of the Amazon, or for rivers draining mountain belts of average crustal composition. In smaller catchments, that possibly contain mafic rocks or carbonates with lower $[^{9}Be]_{parent}$, and on the pedon scale, its validity depends

on the heterogeneity of lithologies in those areas. In such smaller-scale studies $[^9Be]_{parent}$ and its variability will have to be determined on a case-by-case basis by sampling bedrock.

There is a characteristic time scale over which a steady state $(^{10}Be/^{9}Be)_{reac}$ is established. Even though erosion rate, the solute flux, and $F_{met}^{^{10}Be}$ are unlikely to be constant with time, we can still assume that over the weathering time scale, some quasi steady state is established in which such temporal variations average out. Over this time scale, defined in section 2, the characteristic $(^{10}Be/^{9}Be)_{reac}$ is established. A quasi steady state will be achieved if the time scale in temporal variations in of *E* are ca. four to five times shorter than the denudation time scale, or the residence time of ^{10}Be in the weathering zone (Willenbring and von Blanckenburg, 2010b).

There is a characteristic time scale over which $(^{10}Be/^{9}Be)_{diss}$ and $(^{10}Be/^{9}Be)_{reac}$ equilibrate. We assume that $(^{10}Be/^{9}Be)_{diss}$ and $(^{10}Be/^{9}Be)_{reac}$ are equal, as long as changes in *Q* are sufficiently slow to allow for equilibration between Be_{diss} and Be_{reac}. Equilibration times between dissolved and adsorbed Be have been determined to be about a day for the easily exchangeable sites (You et al., 1989), and 10-20 days for the less accessible sites (You et al., 1989; Aldahan et al., 1999; Taylor et al., 2012). This equilibration time is fast and ensures that in most soils, except those that are strongly and temporarily undersaturated in Be_{diss} by rapid rainwater infiltration events, $(^{10}Be/^{9}Be)_{reac}$ and $(^{10}Be/^{9}Be)_{diss}$ have equilibrated and are in a quasi steady state with respect to their fluxes. These assumptions can be tested by several means: at equilibrium, the ratio of $[Be]_{diss}$ and $[Be]_{reac}$ is that of the predicted K_d at the given hydrochemical conditions; $(^{10}Be/^{9}Be)_{reac}$ and $(^{10}Be/^{9}Be)_{diss}$ are identical; and $(^{10}Be/^{9}Be)_{reac}$ does not differ between grain sizes. We will present examples of such tests on the on the Amazon basin in section.

There is a characteristic spatial scale over which steady state $(^{10}Be/^{9}Be)_{reac}$ and $(^{10}Be/^{9}Be)_{diss}$ are established. This spatial scale is one in which variations in the isotope ratio are averaged-out and homogenised by mixing of sediment or water, so that the fluxes into and out of the system are balanced (Fig. 1). At the early stage of this method it is very difficult to predict the scale at which this condition is fulfilled. At the pedon scale, Be isotope ratios vary with depth (Barg et al., 1997), and the way in which they vary at the surface will depend on the structure of underlying soils, determining release and adsorption of isotopes. We can therefore speculate that the minimum spatial scale is the hillslope scale at which lateral and vertical heterogeneities balance out.

Radioactive decay of ^{10}Be is negligible. In the weathering zone, this condition is fullfilled in all settings where E > 1mm kyr^{-1}, depending on the depth of ^{10}Be penetration (Willenbring and von Blanckenburg, 2010b). This is the case in most erosional settings. For radioactive decay to Be or not to be a factor the question is whether sediment is stored in floodplains for > 0.5 My and is also stored over a depth at which no further flux of ^{10}Be is received. This case will only occur in continent-scale drainage basins in which the sediment discharge is also low (see online supplement S3 for a quantification of the change on $(^{10}Be/^{9}Be)_{reac}$) during storage in a floodplain.

Reactive ^{10}Be and ^{9}Be can be extracted from bulk soil and sediment. It is fortunate that existing methods allow the extraction of $^{10}Be_{reac}$ and $^{9}Be_{reac}$ and their separation from $^{9}Be_{min}$ in an operational approach. Be_{reac} is typically extracted by sequential leaching techniques involving weak acids for desorption and dissolving non-crystalline precipitates, reducing agents dissolve crystalline iron oxy-hydroxides (Bourlès et al., 1989; Brown et al., 1992a), and Na-bisulfate to fuse pedogenic clays (Barg et al., 1997). $[^9Be]_{min}$ is typically measured by complete HF dissolution of the previously leached sample. For our Amazon study we present and test such extraction strategies in Wittmann et al. (2012).

The fraction ^{9}Be $\left(f_{reac}^{^{9}Be} + f_{diss}^{^{9}Be}\right)$ released upon weathering can be determined. There are two independent means to determine this parameter that is essential to using eq. (9). The first is independently determining the fractional fluxes in eq. (6) by multiplying water discharge *Q* with $[^9Be]_{diss}$ and dividing by the total ^{9}Be flux

to determine $f_{diss}^{^9Be}$. To determine $f_{reac}^{^9Be}$ and $f_{min}^{^9Be}$ sediment discharge is multiplied with $[^9Be]_{reac}$ and $[^9Be]_{min}$ and divided by the total ^{9}Be flux. Examples for these estimates are shown in the next section for the Amazon basin and are summarised in Table 2. In watersheds where such data is not available, and on the soil scale, these fractions can be determined from samples directly by using $[^9Be]_{reac}$ and $[^9Be]_{min}$ in equations (10) to (13). This approach is likely to work particularly well on soil samples, where particles are not affected by sorting, provided that it can be shown that topsoil $(^{10}Be/^9Be)_{reac}$ integrates over all the processes that are likely to lead to variable $(^{10}Be/^9Be)_{reac}$ at depth. In rivers, $[^9Be]_{reac}$ is potentially enriched over $[^9Be]_{min}$ in the fine fraction by sorting. However, such effects can be corrected for by using ratios of Be to other elements (Wittmann et al., 2012).

4. ^{10}Be/^{9}Be ratios in the Amazon and Orinoco basins

We now explore and test whether the mass balance and the assumptions this new system is based on provide internally consistent degrees of weathering and denudation rates in a well-known field setting. We adopt the "large river approach" in which heterogeneities in sources and fluxes are assumed to be averaged-out. The Amazon basin is ideally suited to perform such a field test: (1) the basin is of a size such that the assumption of average crustal $[^9Be]_{parent}$ (Table 1) is most likely fulfilled; (2) the size of the basin similarly makes the assumption of spatially averaged $F_{met}^{^{10}Be}$ likely. We use $F_{met}^{^{10}Be}$ of 0.8 atoms cm^{-2} yr^{-1} as basin average as derived from the flux map of Willenbring and von Blanckenburg (2010b); (3) denudation rates span a wide range ranging from 2000 t km^{-2} yr^{-1} in the Andes to 30 t km^{-2} yr^{-1} in the stable cratons of the Guyana and the Brazilian Shield; (4) the chemical composition of water in the tributaries is highly diverse (Gaillardet et al., 1997); (5) $(^{10}Be/^9Be)_{reac}$ and $(^{10}Be/^9Be)_{diss}$ are available from the study of Brown et al. (1992a) which is complemented by new data here and in Wittmann et al. (2012) (see online supplement Table 1); (6) independent control over denudation rates is available from *in situ*-produced cosmogenic nuclides (Wittmann et al., 2009; Wittmann et al., 2011).

4.1 Hydrochemical characteristics and sediment fluxes

The Amazon basin comprises an area of 6.1× 10^6 km^2 and a discharge of 6590 km^3 y^{-1}. The Beni, Napo, Mamoré, and Grande tributaries all drain the Andes mountain chain where denudation rates are high with 300 to 2000 t km^{-2} y^{-1} (Wittmann et al., 2009; Wittmann et al., 2010). The Negro River, fed by the Branco tributary, and the Tapajos River drain the Guyana and the Brazilian shields, respectively, where denudation rates are low at 25 to 100 t km^{-2} yr^{-1} (Wittmann et al., 2011). Weathering of the Guyana Shield is deep, extensive, and weathering rates are exceptionally low (Edmond et al., 1995). All these sources of sediment and water mix in the Amazon drunk stream, from which 600 × 10^6 t yr^{-1} of sediment are discharged into the Atlantic (Wittmann et al., 2011). A substantial area of the Guyana Shield also discharges into the Orinoco Basin (area of 1.1× 10^6 km^2, Q is 1135 km^3 yr^{-1}, (Latrubesse et al., 2005)), of which the Apure is a major tributary.

4.2 Grain size dependence

Figure 4a shows $[^{10}Be]_{reac}$ on six grain size fractions of the Beni, the Amazon trunk steam, the Branco, and the Guaporé rivers. Denudation rates of these basins decrease respectively in this order, and $[^{10}Be]_{reac}$ increases concomitantly as expected from eq. (4). However, within each sample $[^{10}Be]_{reac}$ decreases by *ca.* one order of magnitude as the grain size increases from <30 to 125 μm (Fig. 4a).

In contrast, $(^{10}Be/^9Be)_{reac}$ is roughly uniform with grain size for each set of samples, and ratios decrease smoothly with increasing denudation rate (Fig. 4b). Adsorption of ^{10}Be mimics that of ^{9}Be, and retentivity

and grain size effects are cancelled-out through the normalization: $(^{10}Be/^{9}Be)_{reac}$ can be used to determine denudation rates.

4.3 Equilibrium between $(^{10}Be/^{9}Be)_{reac}$ and $(^{10}Be/^{9}Be)_{diss}$

The early Amazon-Orinoco study (Brown et al., 1992a) allows to compare $(^{10}Be/^{9}Be)_{reac}$ with $(^{10}Be/^{9}Be)_{diss}$ (Fig. 5). In seven out of ten samples these two ratios agree to less than a factor of 2, showing near-complete equilibration in the river, and in the remaining three samples the ratios still agree within a factor of 2 – 5. We find this high degree of agreement almost astonishing, as there are several reasons why this might not be the case: (1) samples have been taken in different decades and (2) at different locations (Brown et al., 1992a; Wittmann et al., 2012). (3) These large rivers are subject to complex hydrodynamic behavior, and neither water (Bouchez et al., 2010) nor sediment is necessarily well-mixed. Variability in sediment source manifests itself in grain size-dependent variations (Bouchez et al., 2011) and even in seasonal variations (Viers et al., 2008). (5) Even if samples originating from different sources are well-mixed, mixing times between water and sediment might not have been of sufficient duration to allow for equilibration of Be isotopes.

The overall good agreement between reactive and dissolved $^{10}Be/^{9}Be$ confirms that Be is mostly equilibrated within the residence time of particles in the river, and that a denudation rate can be calculated from both dissolved and reactive Be according to eq. (9) or (10). Furthermore, the uniform nature of $(^{10}Be/^{9}Be)_{reac}$ between grain sizes for a given sample confirms that in these samples equilibrium between dissolved and reactive Be has been established.

4.4 Amazon basin denudation rates

We plot our new $(^{10}Be/^{9}Be)_{reac}$ ratios from the Amazon basin in a diagram constructed from eq. (9) (Fig. 6). To validate the dependence of $(^{10}Be/^{9}Be)_{reac}$ on denudation rate we plot this ratio against the denudation rate determined on the same samples independently using *in situ*-produced ^{10}Be in quartz (Wittmann et al., 2009, 2011). $(^{10}Be/^{9}Be)_{reac}$ ratios are well anti-correlated with D, which ranges from 20 to 2000 t km^{-2} yr^{-1}, and plot within a range of $f_{reac}^{^{9}Be} + f_{diss}^{^{9}Be}$ of between 0.1 and 1. This fact confirms that, to a first order, the assumptions listed above are fulfilled and that most samples are consistent with yielding steady state $(^{10}Be/^{9}Be)_{reac}$ ratios as a function of D. $(^{10}Be/^{9}Be)_{reac}$ is high in the slowly-denuding Guyana and Brazilian Shield rivers. As expected from D provided by *in situ*-produced ^{10}Be, the $(^{10}Be/^{9}Be)_{reac}$ ratio is low in Andean tributaries, featuring high denudation rates, and the Amazon trunk stream, in which the sediment is dominated by Andean sources (Gibbs, 1967; Meade et al., 1985; Wittmann et al., 2011).

Not only do the $(^{10}Be/^{9}Be)_{reac}$ ratios agree with the expected denudation rates. Also $f_{reac}^{^{9}Be} + f_{diss}^{^{9}Be}$ follows the expectations from weathering kinetics. In the Guyana Shield rivers this value is high at 0.6 to 1.0. This high degree of Be released from bedrock is validated independently when using measured fluxes, where $f_{reac}^{^{9}Be} + f_{diss}^{^{9}Be}$ on the Negro is almost 1.0 (Table 2). These values can be expected as in this area the degree of weathering is high and weathering fluxes are likely to be limited by the supply of fresh minerals to the weathering zone (Edmond et al., 1995). In Andean sediment, in contrast, $f_{reac}^{^{9}Be} + f_{diss}^{^{9}Be}$ is much lower, at 0.1 to 0.4. Again, agreement between $f_{reac}^{^{9}Be} + f_{diss}^{^{9}Be}$ from river fluxes (Table 2) and Fig. 6 is excellent. A low degree of weathering is expected in these rapidly denuding sediment source areas as in these settings, the dissolution of primary minerals is incomplete and therefore reaction kinetics set mineral weathering fluxes (Stallard and Edmond, 1987). Note that $(^{10}Be/^{9}Be)_{reac}$ in our Negro sample is lower than in Guyana shield rivers, while D from *in situ*-produced ^{10}Be is higher, and consequently, our modeled $f_{reac}^{^{9}Be} + f_{diss}^{^{9}Be}$ appears to be too low when compared with the flux-based estimate from Table 2. This discrepancy can be explained

with entrainment of Andean-sourced bed sediment into the Negro basin at this particular site that is close to the confluence with the Solimões (Wittmann et al., 2011), where these two rivers join to form the Amazon River. The Negro sample would therefore represent a perfect binary mixture between the shield and the Andean sediment source. The minor increase in $(^{10}Be/^{9}Be)_{reac}$ of Brazilian Shield values over a ratio expected from weathering kinetics (with probably high $f_{reac}^{^{9}Be} + f_{diss}^{^{9}Be}$) can potentially be explained by shallow intermittent storage (see online supplement S.3 for a quantification of this effect). Overall, our Amazon data show that denudation rates *D* and degree of chemical weathering can be calculated from $(^{10}Be/^{9}Be)_{reac}$ or $(^{10}Be/^{9}Be)_{diss}$ in large river basins.

5. Denudation rates from ^{10}Be/^{9}Be in large rivers

We proceed to test how *D* from ^{10}Be/^{9}Be on a wide range of global rivers compares with *D* from independent estimates. In Fig. 7 we plot *D* calculated from $(^{10}Be/^{9}Be)_{reac}$ or $(^{10}Be/^{9}Be)_{diss}$ using eq. (9) and using the parameters given in the figure caption. We use $(^{10}Be/^{9}Be)_{diss}$ from Amazon basin rivers (Brown et al., 1992a), Northwest USA rivers (Kusakabe et al., 1991), and Arctic rivers (Frank et al., 2008). Where available, we compare these to *D* from the sum of suspended and dissolved fluxes reported for these rivers by Milliman and Farnsworth (2011). We also compare $(^{10}Be/^{9}Be)_{reac}$ for the new Amazon data given in this study to *D* (section 4) from *in situ*-produced cosmogenic nuclides (Wittmann et al., 2011).

We do not know $f_{reac}^{^{9}Be} + f_{diss}^{^{9}Be}$ for each of these rivers. However, a fit through all data shows that these obey a global mean of 0.2. This value is similar to the $f_{reac}^{^{9}Be} + f_{diss}^{^{9}Be}$ of 0.26 that was measured for for the Amazon river (Table 2). With only two exceptions (Cb samples from the Brazilian Shield discussed in online supplement S.3, and the Klamath river, draining in part basaltic rocks with lower $[^{9}Be]_{parent}$), the data fall within a range that is compatible with $f_{reac}^{^{9}Be} + f_{diss}^{^{9}Be}$ being half or double the global value of 0.2 (thin grey lines bracketing this range in Fig. 7).

Overall, the denudation rates calculated from both dissolved and reactive ^{10}Be/^{9}Be agree within a factor of two with the independent estimates. We find this agreement extremely encouraging, and suggest that the new ^{10}Be/^{9}Be method is suited to provide a rapid and accurate estimate of denudation from the dissolved or the solid load of rivers.

6. Discussion and conclusions

We have presented a series of predictions for the way the isotope ratio ^{10}Be/^{9}Be is controlled by denudation and weathering on the soil scale to the river basin scale. We summarise these hypotheses here and suggest tests of the assumptions the method is based on.

1) The single-isotope system ^{10}Be(meteoric) is suited to determine an erosion rate *E* from bulk soil samples using total soil or adsorbed ^{10}Be concentration, provided that the ratio of discharge to partition coefficient is much smaller than the erosion rate. In river sediment, an erosion rate *E* cannot easily be calculated from ^{10}Be concentrations as these concentrations are highly grain size-dependent following riverine sorting.
2) At steady state, meaning that variations in fluxes average out over several denudational time scales (typically several 10^3-10^5 yr), the ^{10}Be/^{9}Be ratio of "reactive" Be (*i.e.* adsorbed to particles and incorporated into solid secondary weathering products, not depending on grain size) yields a denudation rate *D*, provided that the fraction of ^{9}Be that is released from primary minerals is known. This fraction can be determined from riverine fluxes or, alternatively, from measuring both the adsorbed and residual mineral-bound ^{9}Be contained in sediment.

3) Dissolved and reactive Be equilibrate provided that the contact time between water and particles is sufficiently long, *D* can also be determined from dissolved Be in river water. More field and laboratory experiments are required, however, to determine under which hydrochemical compositions, properties of the solids, and time scales this equilibrium is established.
4) There is a characteristic spatial scale above which local heterogeneities in $^{10}Be/^{9}Be$ cancel out so that at this scale the fluxes of these two isotopes in and out of the weathering zone are at steady state. This characteristic scale needs to be determined. We speculate that this scale is at least that of the hillslope, where all lateral and vertical heterogeneities in the distribution of both isotopes of Be by soil physical properties average out, or that of a small river basin.
5) Knowing the ^{9}Be concentration of parent rock is required for calculating *D*. At large scale, where lithology approaches that of average crustal rock, this concentration is 2.5 ± 0.5 ppm. At the spatial scales of the soil column, the hillslope, or a small watershed, this concentration needs to be determined from measuring bedrock concentrations.

In any case knowing the atmospheric flux of ^{10}Be is required for using both the single-isotope ^{10}Be method and the $^{10}Be/^{9}Be$ method. Over the denudational time scale temporal variations in this flux are likely to cancel out. Over the large spatial scale, this flux can be read from global flux maps. Over the small spatial scale, this flux potentially depends on short-scale orographic and other differences in precipitation. Future work should provide better models and data of the local distribution of the atmospheric ^{10}Be flux are required.

All of these hypotheses and assumptions require rigorous testing in both field and laboratory studies. Yet the initial tests of the method on the Amazon basin and measurements on global rivers yield very encouraging results. When applied to the authigenic phase of the sedimentary record, we expect that this method will indeed provide past denudation rates from river, lake, or ocean sediment as suggested for the Late Cenozoic by Willenbring and von Blanckenburg (2010a).

Acknowledgements

We are grateful to Nadine Dannhaus for contributing to the Amazon data, Jane Willenbring for inspirations on meteoric ^{10}Be and global erosion rates, Jean Dixon for a first internal review, and Manuela Dziggel for drafting Fig. 1. We thank Darryl Granger, John Stone, and two anomymous reviewers for their careful reviews.

Appendix

A.1. Quantifying the bias on *E* introduced by loss of ^{10}Be to solution

The single-isotope system ^{10}Be is compromised by the condition of quantitative retentivity. Quantitative retentivity in the sense of equation (3) is established when Q is low or E is high or K_d is high such that $Q/K_d << E$. Since an approximate ratio of Q/E can be predicted for a given field setting, we express this condition as :

$$\frac{Q}{E} \ll K_d \qquad \text{(A1)}$$

in which case eq. (3) simplifies to:

$$E = \frac{^{10}F_{met}^{Be}}{[^{10}Be]_{reac}} \qquad \text{(A2)}$$

Fortunately, in many settings condition (A1) can be evaluated, as rough estimates of Q are mostly known, and K_d can be measured in a retention experiment or estimated from soil or river pH. We quantify the bias (in %) introduced by this simplification by the relative difference in calculated E using the simplified eq. (4) instead of the accurate eq. (3):

$$\frac{bias}{[\%]} = \frac{Q}{E*K_d} * 100 \quad \text{(A3)}$$

This bias is shown in Fig. A.1a. ^{10}Be retention is high and eq. (4) is adequate in settings where E is high and Q is low, or when soil- and river $K_d > 10^5$ L kg^{-1}, corresponding to a pH > 6 (You et al., 1989; Aldahan et al., 1999). For soils, unless they are buffered by equilibrium with carbonate minerals, this latter condition is rarely fulfilled. Even in active mountain belts, where E is high, retention behavior might be an issue as at these sites also precipitation is usually high. In tropical shield areas, where E is low and precipitation is high, Be retention will be very low. In this case, basing erosion rates on ^{10}Be concentrations as single isotope tracer is likely to strongly overestimate erosion rates. For these systems, knowing Q and K_d values is a requirement for accurate estimates of E from using $[^{10}Be]_{reac}$.

A.2. Quantifying the bias on D from $(^{10}Be/^{9}Be)_{reac}$ introduced by ignoring the Q/K_d term in equation (12) and (13)

Although mathematically $(^{10}Be/^{9}Be)_{reac}$ or $(^{10}Be/^{9}Be)_{diss}$ do not depend on Q or K_d, in practice, determining D from $(^{10}Be/^{9}Be)_{reac}$ or $(^{10}Be/^{9}Be)_{diss}$ using eq. (10) and (11) requires knowing $\frac{Q}{K_d}$. This issue can be resolved if $f_{reac}^{^{9}Be} + f_{diss}^{^{9}Be}$ is known from independent means. If this is not possible, the simplification can still be made if the entire denominator in eqs. (10) and (11) approaches unity so that:

$$\frac{Q*[\,^{9}Be]_{min}}{D*[\,^{9}Be]_{parent}} \ll K_d \quad \text{(A4)}$$

which is equivalent to:

$$\frac{Q}{E} * f_{min}^{^{9}Be} \ll K_d \quad \text{(A5)}$$

Then D can be calculated by ignoring the $\frac{Q}{K_d}$ term, leading to equations (12) and (13).

The bias in denudation rate (in %) resulting from using the simplified eqs. (12) and (13) rather than the accurate equation (10) and (11) is:

$$\frac{bias}{[\%]} = \frac{Q*[\,^{9}Be]_{min}}{K_d*D*[\,^{9}Be]_{parent}} * 100 = \frac{Q}{E*K_d} * f_{min}^{^{9}Be} * 100 \quad \text{(A6)}$$

In contrast to the single isotope system ^{10}Be, this bias also depends on the distribution of ^{9}Be between the sum of the reactive and the dissolved compartment on the one hand, and the residual $^{9}Be_{min}$ on the other hand (Fig. A1b). At $f_{min}^{^{9}Be}$ of 1, the bias in D resulting from the ^{10}Be/^{9}Be system is identical to that for E for the ^{10}Be system for a given K_d (Fig. A1a). In such a case the degree of weathering is low, and using eqs. (12) and (13) can be highly inaccurate if discharge is high and denudation is low. This case is unlikely to exist very often. Indeed, in high-Q, low-D settings, like tropical shields, $f_{min}^{^{9}Be}$ is likely to be low too, *i.e.* the degree of weathering is high. Then the bias is small regardless of the values of the other parameters Q and K_d. These are exactly the settings where the simplified single ^{10}Be isotope eq. (4) fails (Appendix A.1). Finally, if $f_{min}^{^{9}Be}$ is low, then $[^{9}Be]_{min} << [^{9}Be]_{reac}$ and $(^{10}Be/^{9}Be)_{reac}$ is close to $(^{10}Be/^{9}Be)_{total}$. In this case, determination of D

can be carried out from a measurement of a $^{10}Be/^{9}Be$ ratio measured either in (1) a bulk river sediment, bedload or suspended load (eq. 13); (2) the reactive phase of this river sediment (eq. 12); or (3) a simple sample of filtered river water (eq. 12).

Figures & Tables

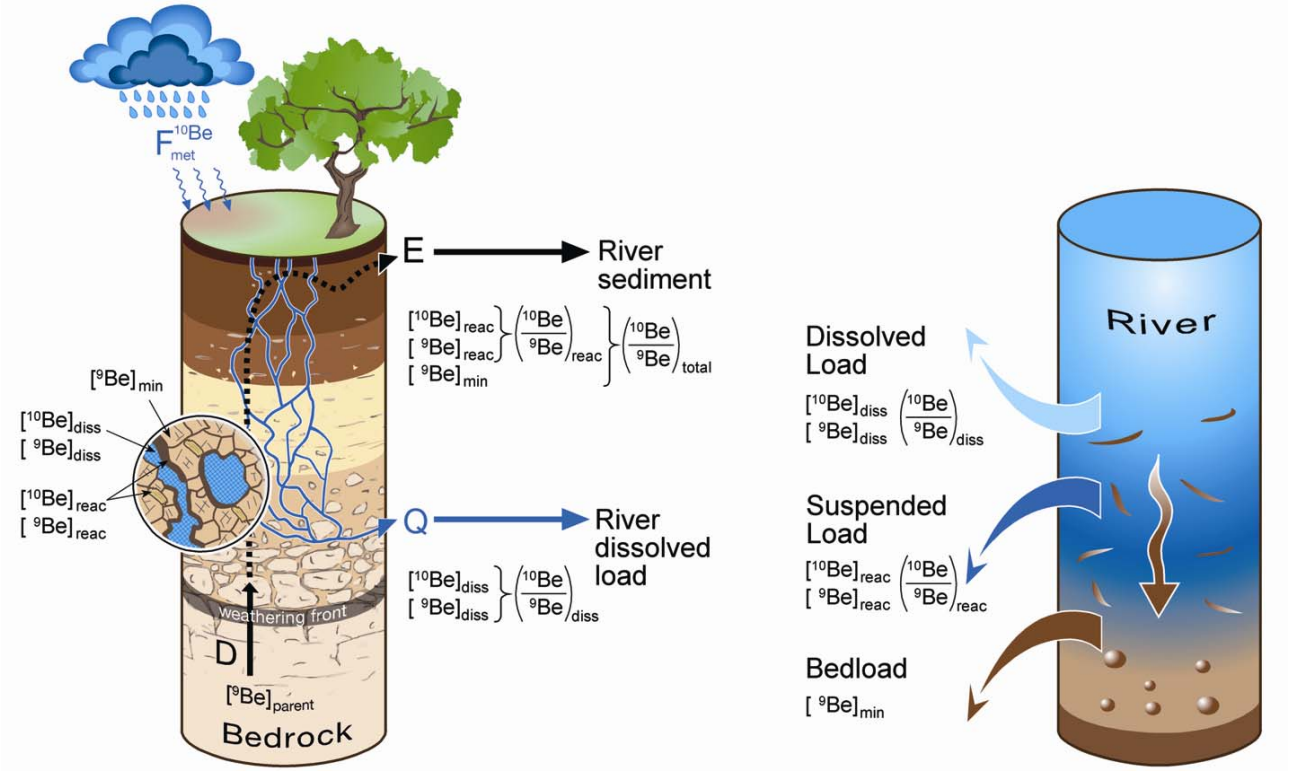

Figure 1: Model weathering system and the fluxes of meteoric ^{10}Be, entering the system by atmospheric fallout, and of ^{9}Be, released during weathering of the parent rock by decomposition of primary minerals (parent). These isotopes are partitioned into a dissolved phase (diss), a reactive phase (reac) such as incorporated into pedogenic clay minerals or into iron oxyhydroxide coatings, and a residual mineral-borne phase (min). Characteristic ^{10}Be/^{9}Be ratios result for each of these compartments. Be_{min} and Be_{reac} leave the weathering zone by erosion (rate *E*), and Be_{diss} leaves the zone by groundwater discharge or runoff (rate *Q*). Mathematically we treat these fluxes as a steady-state "black box", without considering the internal vertical or lateral distribution of isotopes, or changes in their fluxes. Our mass balance approach merely requires that all fluxes balance each other at steady state, which will likely be the case once a site-specific spatial and temporal scale is exceeded. While the main chemical interactions that set the ^{10}Be/^{9}Be ratios take place in the weathering zone (left), the spatial scale at which fluxes balance is likely to be that of a hillslope or that of a small river (right).

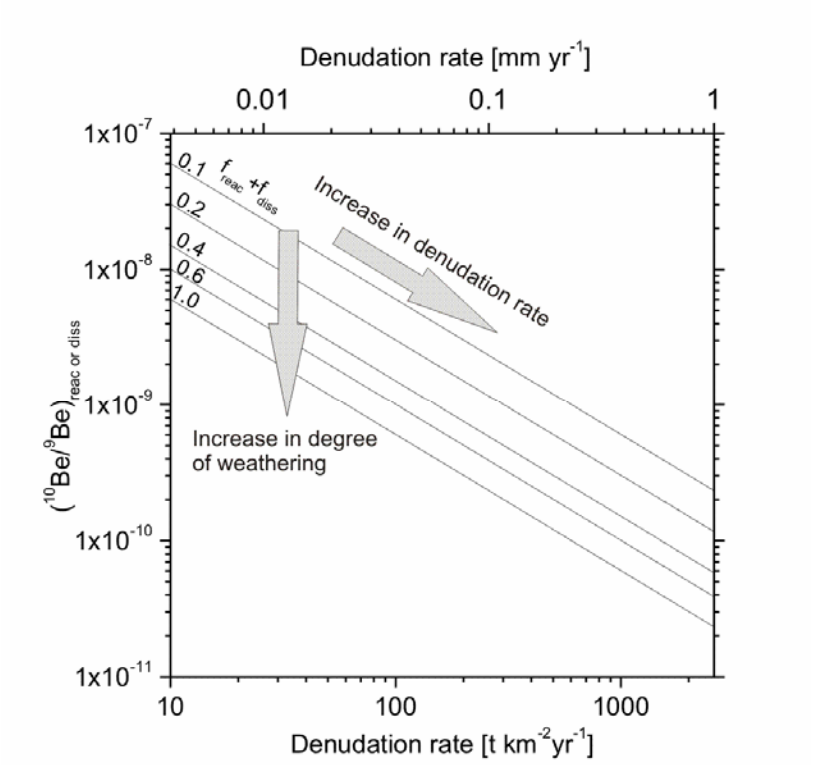

Figure 2: Illustration of the way the $(^{10}Be/^{9}Be)_{reac}$ or $(^{10}Be/^{9}Be)_{diss}$ ratio can be used to infer a denudation rate *D*. Following eq. (9) the isotope ratio also depends on the amount fraction of ^{9}Be contained in the reactive and the dissolved phase $f_{reac}^{\ ^{9}Be} + f_{diss}^{\ ^{9}Be}$ within a river or in soil. Hence the relationship between ^{10}Be/^{9}Be and *D* is shown for a variety of $f_{reac}^{\ ^{9}Be} + f_{diss}^{\ ^{9}Be}$ which ranges from 0.1 (most ^{9}Be still present as $^{9}Be_{min}$) to 1 (all $^{9}Be_{parent}$ unlocked from primary minerals). Since the fraction $f_{reac}^{\ ^{9}Be} + f_{diss}^{\ ^{9}Be}$ is likely to increase with the degree of chemical weathering the resulting ^{10}Be/^{9}Be ratio decreases according to the vertical arrow. The model was calculated using an atmospheric ^{10}Be flux $F_{met}^{\ ^{10}Be}$ of 1 × 10^{6} atoms cm^{-2} yr^{-1}, and a bedrock ^{9}Be concentration $[^{9}Be]_{parent}$ of 2.5 ppm.

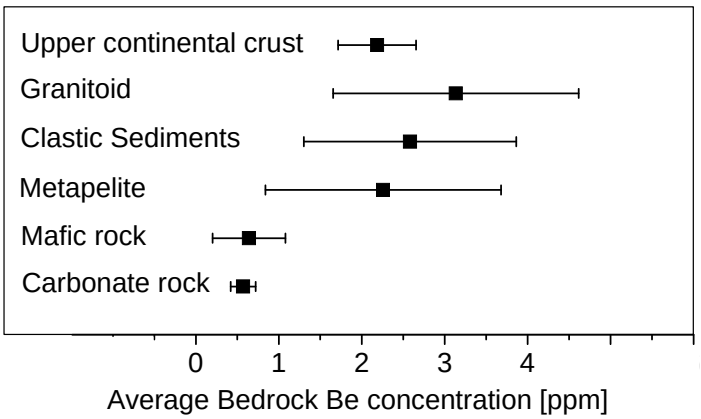

Figure 3: Average Be concentrations of typical parent rocks. At large spatial scale, where lithologic types average out, a $[^{9}Be]_{parent}$ of 2.5 ppm can be inferred. See Tab.1 for data sources.

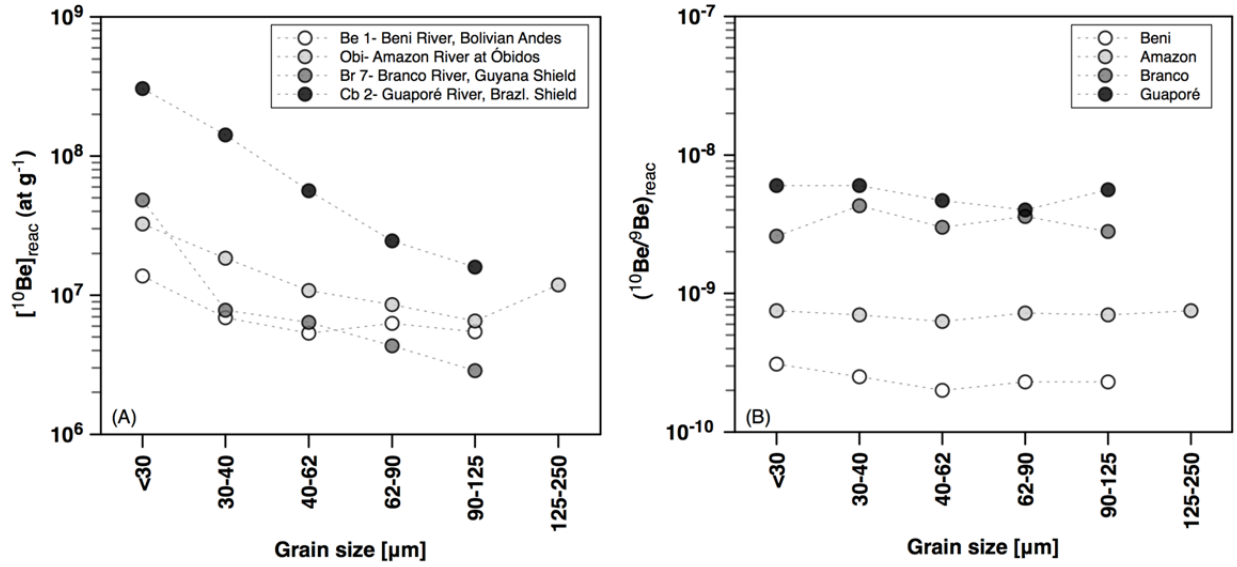

Figure 4: Comparison of $[^{10}Be]_{reac}$ and $(^{10}Be/^{9}Be)_{reac}$ in the fine fraction of sediment in the Amazon basin. The reactive Be was obtained by combining sequential extractions of 0.5M HCl, followed by 1M hydroxylamine in 1M HCl, respectively (Wittmann et al., 2012). While $[^{10}Be]_{reac}$ is strongly grain size-dependent, $(^{10}Be/^{9}Be)_{reac}$ does not vary with grain size. Denudation rates from *in situ*-produced ^{10}Be in quartz on these sediment samples are 0.36 mm yr^{-1} for sample Be 1, 0.22 mm yr^{-1} for sample Obi, 0.014 mm yr^{-1} for sample Br 7, 0.021 mm yr^{-1} for sample Cb 2 (Wittmann et al., 2011), corresponding to *D* of 940, 570, 36, and 55 t km^{-2} yr^{-1} when converted using a density of 2.6 t m^{-3}.

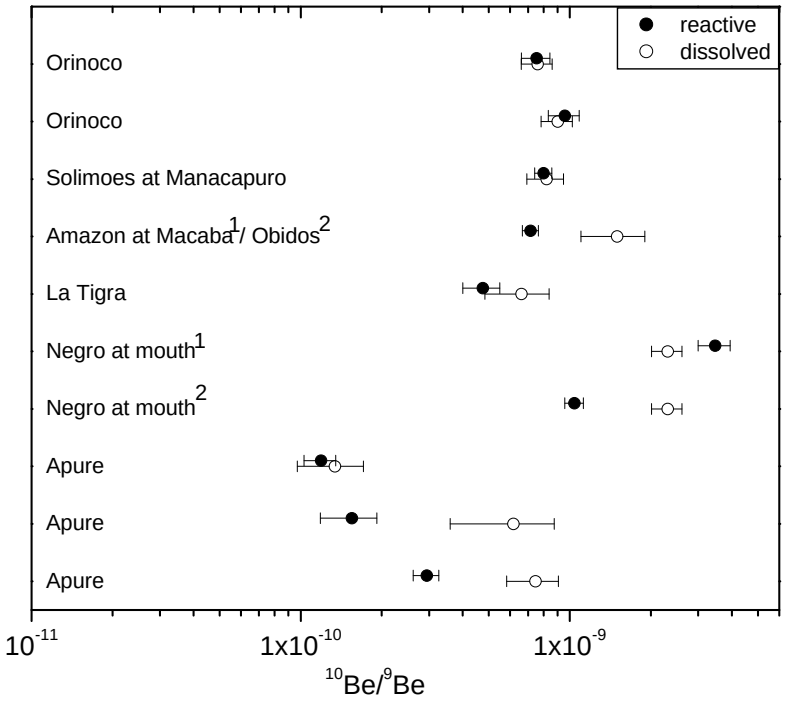

Figure 5: Comparison of leached $(^{10}Be/^{9}Be)_{reac}$ with dissolved $(^{10}Be/^{9}Be)_{diss}$ ratios in the Orinoco and Amazon basin (Brown et al., 1992a). Data denoted by "1" shows reactive Be measured by Brown for the same dissolved sample, whereas "2" shows additional reactive Be (Wittmann et al., 2012).

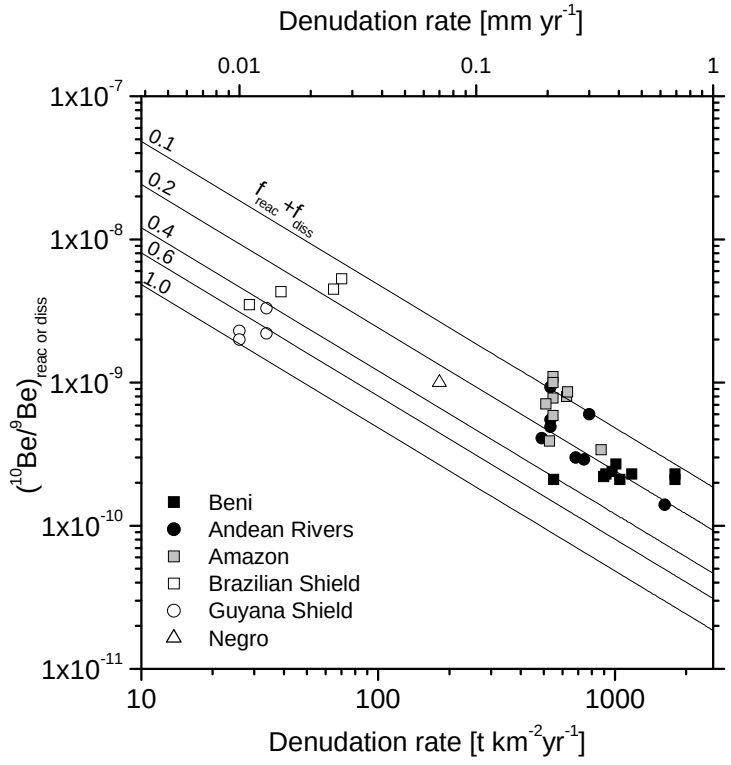

Figure 6: Test of measured $(^{10}Be/^{9}Be)_{reac}$ obtained from leaching fine-grained river sediment in the Amazon and its tributaries (Wittmann et al., 2012) against denudation rates obtained independently from *in situ*-produced ^{10}Be in quartz from the same samples (Wittmann et al., 2009; Wittmann et al., 2011). Contour lines are the same as in Fig. 2, except for F_{met}^{10Be} that was adjusted to a mean value of 0.8 x10^{-6} atoms cm^{-2} yr^{-1} for the Amazon basin (Willenbring and von Blanckenburg, 2010b). Note that overall $(^{10}Be/^{9}Be)_{reac}$ is well inversely correlated with denudation rate and falls within the array predicted by eq. (9). Furthermore, samples dominated by Andean erosion products, like the Beni, the Amazon trunk stream, and other Andean rivers plot on lines of low $f_{reac}^{9Be} + f_{diss}^{9Be}$ whereas Guyana Shield rivers are more compatible with high $f_{reac}^{9Be} + f_{diss}^{9Be}$. This behaviour is expected, as the degree of weathering is low in the Andes, and high in tropical shield areas. In online supplement 3 we show the potential change in $(^{10}Be/^{9}Be)_{reac}$ during sediment storage. See supplementary tables for data sources.

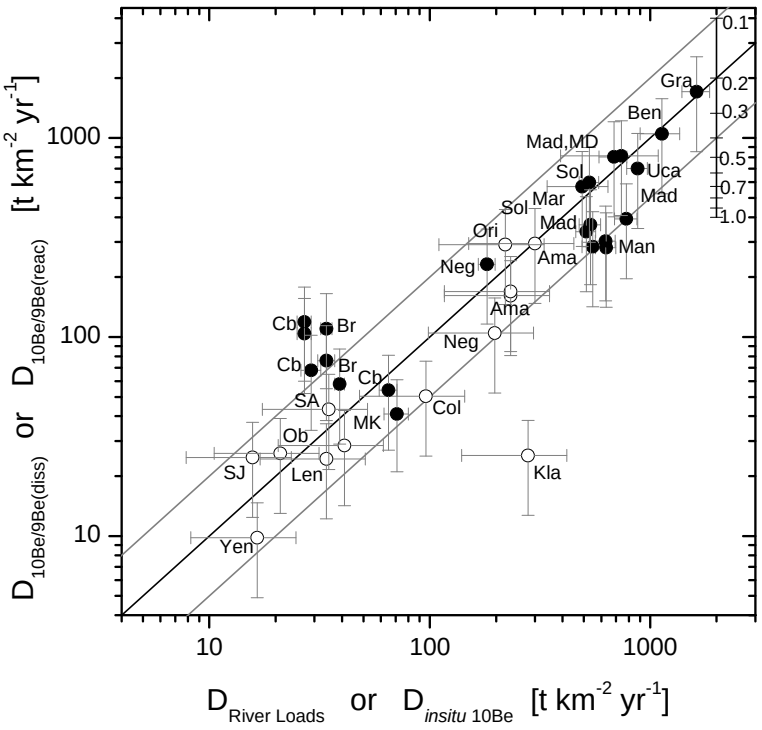

Figure 7: Comparison of catchment-wide denudation rates *D* calculated from $^{10}Be/^{9}Be$ using eq. (9) for those global rivers for which an estimate of denudation rate with an independent method is available. For open symbols, $D_{10Be/9Be(diss)}$ was calculated from $(^{10}Be/^{9}Be)_{diss}$ data for North USA rivers from Kusakabe et al., (1991): Col: Columbia; SA: Santa Ana; Kla: Klamath; SJ: San Joaquin. Arctic rivers are from Frank et al., (2008): Len: Lena; MK: Mac Kenzie; Yen: Yenisei; Ob. South American rivers are from Brown et al. (1992): Ama: Amazon; Neg: Negro; Ori: Orinoco; Sol: Solimões. *D* on the x-axis is from river suspended and dissolved loads (from Milliman and Farnsworth (2011), except for the Solimoes at Manaus that is from Wittmann et al. (2011). Closed symbols: $D_{10Be/9Be(reac)}$ was calculated from $(^{10}Be/^{9}Be)_{reac}$ from bedload samples from the Amazon basin (Wittmann et al., 2012). Cb: Brazilian Shield samples; Br: Branco; Gra: Grande; Mad: Madeira; MD: Madre de Dios; Be: Beni; Uca: Ucayali; Mar: Mamoré; Man: Solimões at Manacapura; Ama: Amazon at Obidos, Parintins, and Iracema, respectively. *D* on the x-axis is from *in situ*-produced cosmogenic ^{10}Be measured in quartz on river bedload (Wittmann et al., 2011) for the same samples on which $(^{10}Be/^{9}Be)_{reac}$ was determined. Error estimates are ± 50% for *D* from river loads (taking into account an estimate for the differences that are commonly found when the decadal time scale estimates of suspended loads are compared with the millenial time scales for cosmogenic nuclides). Errors on *D* from *in situ*-produced ^{10}Be are the individual errors that were reported for these estimates. Error on *D* from meteoric $^{10}Be/^{9}Be$ are estimated to be ± 50%, broadly combining errors in estimates of $F_{met}^{^{10}Be}$ and $[^{9}Be]_{parent}$. Where multiple $^{10}Be/^{9}Be$ measurements are available for one river the resulting individual *D*'s were averaged. $D_{10Be/9Be}$ was calculated using the individual basins $F_{met}^{^{10}Be}$ from Willenbring and von Blanckenburg (2010b); $[^{9}Be]_{parent}$ of 2.5 ppm, and an $f_{reac}^{^{9}Be} + f_{diss}^{^{9}Be}$ of 0.2. The black line shows the 1:1 slope of the two estimates, and the grey lines show the 1:2 and 2:1 slopes, respectively. The scale bar on the upper right shows how *D* determined from $^{10}Be/^{9}Be$ would change for a given data point if $f_{reac}^{^{9}Be} + f_{diss}^{^{9}Be}$ would be different from the assumed value of 0.2. See online supplementary Table 2 for raw data used.

Table 1: Average bedrock Be concentrations

	Conc. [ppm]	Std.dev. [ppm]	No of data sets
Upper Continental Crust	2.2	0.5	16
Granitoids	3.1	1.5	10
Clastic Sediments	2.6	1.3	30
Metapelites	2.3	1.4	11
Mafic Rocks	0.64	0.44	11
Carbonates	0.57	0.15	2

Average Be concentrations in rocks as compiled from the mean given in previous compilations (Grew, 2002) [http://earthref.org/GERM; July 2011 (Staudigel et al., 1998)]. Note that each of the entries denoted by the count given averages over *ca*. 10 to 1000 individual measurements.

Table 2: Measured fraction of ^{9}Be

Sample	$f_{diss}^{^{9}Be}$	$f_{reac}^{^{9}Be}$	$f_{min}^{^{9}Be}$	$f_{reac}^{^{9}Be} + f_{diss}^{^{9}Be}$
Amazon at Macapa/Obidós	0.029	0.23	0.74	0.26
Solimoes at Manaus	0.018	0.11	0.87	0.13
Negro at Manaus	0.65	0.29	0.06	0.94
Amazon Andean Rivers	0.002	0.29	0.71	0.29
Beni	0.001	0.31	0.69	0.31

$f_{diss}^{^{9}Be}$ was calculated from $[^{9}Be]_{diss}$ (Brown et al. (1992a) multiplied by water discharge Q (see supplementary table 1 for data sources). $f_{reac}^{^{9}Be}$ and $f_{min}^{^{9}Be}$ were calculated from $[^{9}Be]_{reac}$ and $[^{9}Be]_{min}$ from Brown et al. (1992) (Negro), and Wittmann et al. (2012) (Beni, Amazon at Obidós) and all other rivers according to the online supplement and were multiplied by suspended sediment flux (Wittmann et al., 2011). Note that $[^{9}Be]_{diss}$ for the Amazon is from Macapa, whereas $[^{9}Be]_{reac}$ and $[^{9}Be]_{min}$ are from Obidós. Note also that no $f_{diss}^{^{9}Be}$ is available for the Beni and the other Andean rivers. Instead $[^{9}Be]_{diss}$ was taken from the Caparo and Canagua rivers (samples 810 and 808, Brown et al. 1992), and combined with our own measurements of $[^{9}Be]_{reac}$ and $[^{9}Be]_{min}$ for the Beni and the other Andean rivers.

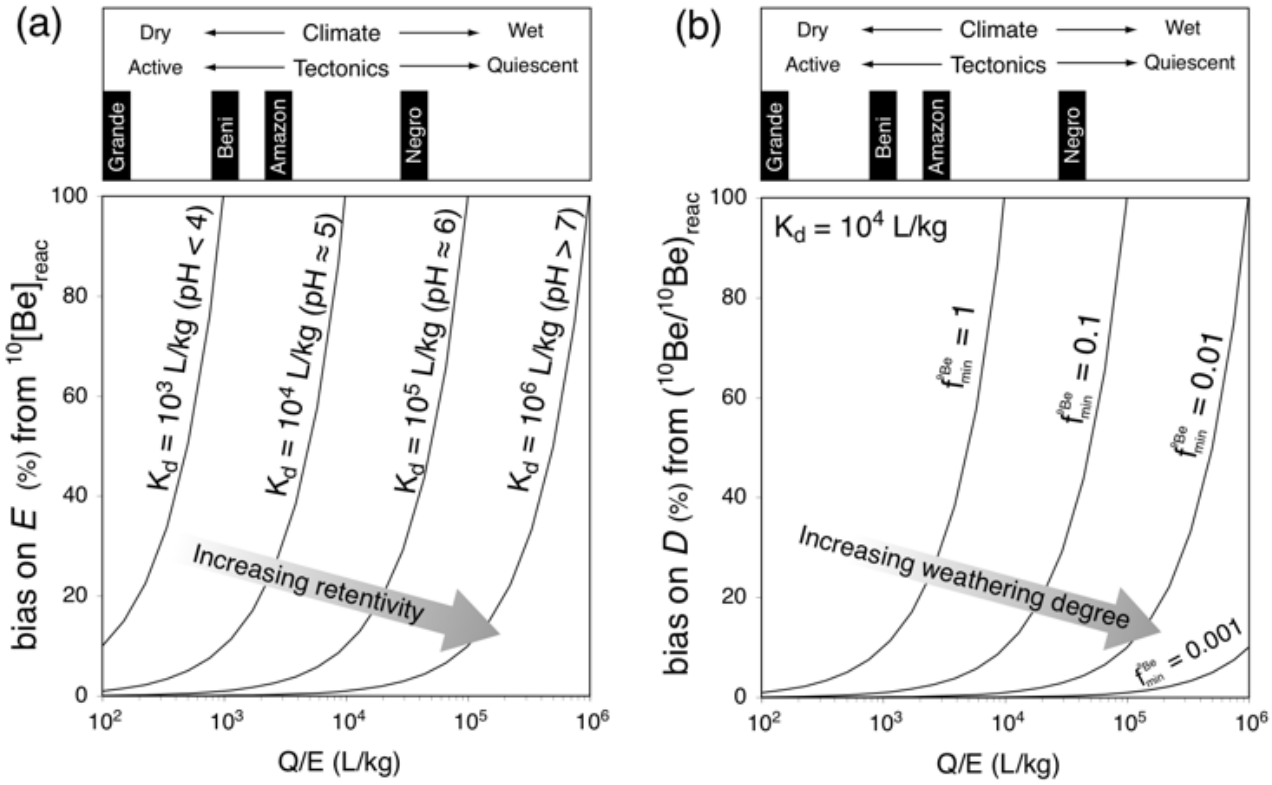

Figure A.1: a) Bias introduced into estimates of *E* (left, from ^{10}Be) when the ^{10}Be lost into solution is ignored, meaning using the simplified eq. (4) instead of the full eq. (3). This bias is calculated using eq. (A3) and depends on the Be partition coefficient (K_d), the water flux *Q*, and the erosion rate *E*. Note that *Q/E* is similar to a fluid/solid ratio during weathering. The bias is calculated for different values of K_d. For example, if $Q/E = 10^4$ L/kg, and $K_d = 10^5$ L/kg (which would correspond to pH = 6 (You et al., 1989; Aldahan et al., 1999)), *E* is overestimated by 10%. B) Bias in *D* (right, from $(^{10}Be/^{9}Be)_{reac}$ or $(^{10}Be/^{9}Be)_{diss}$) using simplified eqs. (12) and (13). The bias on estimates of *D* from the $(^{10}Be/^{9}Be)_{reac}$ or $(^{10}Be/^{9}Be)_{diss}$ is calculated from eq. (A6) and depends on the erosion rate, and also on $f_{min}^{^{9}Be}$ and hence on the degree of weathering. The bias is plotted here for different values of $f_{min}^{^{9}Be}$ and for one value of K_d (10^4 L/kg, corresponding to pH = 5). Lower values of $f_{min}^{^{9}Be}$ imply that more ^{9}Be has been dissolved from the parent rock. Hence the bias in *D* is sensitive to the degree of weathering. The maximum bias in *D* can result for the case where $f_{min}^{^{9}Be} = 1$. In this case the bias in calculating *E* and *D* with the simplified equations are equal; but for lower values of $f_{min}^{^{9}Be}$ (greater weathering degrees), the bias in calculating *D* is always smaller than that resulting from ^{10}Be only. Above the diagram are shown, as examples, the *Q/E* ratios of major sub-basins of the Amazon systems, and how two major controlling factors of *Q/E*, *i.e.* climate and/or tectonics, will play a role in the size of this bias.

References

Aldahan, A., Ye, H.P., Possnert, G., 1999. Distribution of beryllium between solution and minerals (biotite and albite) under atmospheric conditions and variable pH. Chemical Geology 156, 209-229.

Bacon, A.R., Richter, D.D., Bierman, P.R., Rood, D.H., 2012. Coupling meteoric ^{10}Be with pedogenic losses of ^{9}Be to improve soil residence time estimates on an ancient North American interfluve. Geology 40, 1-4.

Barg, E., Lal, D., Pavich, M.J., Caffee, M.W., Southon, J.R., 1997. Beryllium geochemistry in soils: evaluation of ^{10}Be/^{9}Be ratios in authigenic minerals as a basis for age models. Chemical Geology 140, 237-258.

Bouchez, J., Gaillardet, J., France-Lanord, C., Maurice, L., Dutra-Maia, P., 2011. Grain size control of river suspended sediment geochemistry: Clues from Amazon River depth profiles. Geochemistry Geophysics Geosystems 12, Q03008.

Bouchez, J., Lajeunesse, E., Gaillardet, J., France-Lanord, C., Dutra-Maia, P., Maurice, L., 2010. Turbulent mixing in the Amazon River: The isotopic memory of confluences. Earth and Planetary Science Letters 290, 37-43.

Bourlès, D., Raisbeck, G.M., Yiou, F., 1989. ^{10}Be and ^{9}Be in marine sediments and their potential for dating. Geochimica Cosmochimica Acta 53, 443-452.

Brown, E.T., Edmond, J.M., Raisbeck, G.M., Bourles, D., Yiou, F., Measures, C.I., 1992a. Beryllium isotope geochemistry in tropical river basins. Geochim. Cosmochim. Acta 56, 1607-1624.

Brown, E.T., Measures, C.I., Edmond, J.M., Bourles, D.L., Raisbeck, G.M., Yiou, F., 1992b. Continental inputs of Beryllium to the oceans. Earth and Planetary Science Letters 114, 101-111.

Brown, L., Pavich, M.J., Hickman, R.E., Klein, J., Middleton, R., 1988. Erosion of the eastern United States observed with ^{10}Be. Earth Surface Processes and Landforms 13, 441-457.

Chmeleff, J., von Blanckenburg, F., Kossert, K., Jakob, D., 2010. Determination of the ^{10}Be half-life by multicollector ICP-MS and liquid scintillation counting. NIM-B: Beam Interactions with Materials and Atoms 268, 192-199.

Edmond, J.M., Palmer, M.R., Measures, C.I., Grant, B., Stallard, R.F., 1995. The fluvial geochemistry and denudation rate of the Guyana Shield in Venezuela, Colombia, and Brazil. Geochim. Cosmochim. Acta 59, 3301-3325.

Field, C.V., Schmidt, G.A., Koch, D., Salyk, C., 2006. Modeling production and climate-related impacts on ^{10}Be concentration in ice cores. Journal of Geophysical Research 111, doi:10.1029/2005JD006410.

Frank, M., Backman, J., Jakobsson, M., Moran, K., O'Regan, M., King, J., A. Haley, B.A., Kubik, P.W., Garbe-Schönberg, D., 2008. Beryllium isotopes in central Arctic Ocean sediments over the past 12.3 million years: Stratigraphic and paleoclimatic implications. Paleoceanography 23, PA1S02, doi:10.1029/2007PA001478.

Gaillardet, J., Dupré, B., Allègre, C.J., Negrel, P., 1997. Chemical and physical denudation in the Amazon River basin. Chemical Geology 142, 141-173.

Gibbs, R.J., 1967. Amazon River - Environmental Factors that control its dissolved and suspended load. Science 3783, 1734-1737.

Graly, J.A., Bierman, P.R., Reusser, L.J., Pavich, M.J., 2010. Meteoric (10)Be in soil profiles - A global meta-analysis. Geochim. Cosmochim. Acta 74, 6814-6829.

Grew, E.S., 2002. Beryllium in Metamorphic Environments (emphasis on aluminous compositions). Reviews in Mineralogy and Geochemistry 50, 487-549.

Heikkilä, U., Beer, J., Feichter, J., 2008. Meridional transport and deposition of atmospheric ^{10}Be. Atmospheric Chemistry and Physics Discussions 8, 16819-16849.

Jungers, M.C., Bierman, P.R., Matmon, A., Nichols, K., Larsen, J., Finkel, R., 2009. Tracing hillslope sediment production and transport with in situ and meteoric ^{10}Be. Journal of Geophysical Research F04020, doi:10.1029/2008JF001086.

Korschinek, G., Bergmaier, A., Faestermann, T., Gerstmann, U.C., Knie, K., Rugel, G., Wallner, A., Dillmann, I., Dollinger, G., Lierse von Gostomskie, C., Kossert, K., Maitia, M., Poutivtsev, M., Remmert, A., 2010. A new value for the half-life of ^{10}Be by heavy ion elastic recoil detection and liquid scintillation counting Nuclear Instruments and Methods B 268, 187-191.

Kusakabe, M., Ku, T.L., Southon, J.R., Shao, L., Vogel, J.S., Nelson, D.E., Nakaya, S., Cusimano, G.L., 1991. Be isotopes in rivers/estuaries and their oceanic budgets. Earth and Planetary Science Letters 102, 265-276.

Lal, D., 1991. Cosmic ray labeling of erosion surfaces: in situ nuclide production rates and erosion models. Earth and Planetary Science Letters 104, 424-439.
Lal, D., Peters, B., 1967. Cosmic-ray-produced radioactivity on the Earth, Handbuch der Physik. Springer Verlag, Berlin, pp. 551-612.
Latrubesse, E.M., Stevaux, J.C., Sinha, R., 2005. Tropical rivers. Geomorphology 70, 187-206.
Meade, R.H., Dunne, T., Richey, J.E., Santos, U., Salati, E., 1985. Storage and Remobilization of Suspended Sediment in the Lower Amazon River of Brazil. Science 228, 488-490.
Milliman, J.D., Farnsworth, K.L., 2011. River discharge to the coastal ocean. A global synthesis. Cambridge University Press, Cambridge.
Monaghan, M.C., Krishnaswami, S., Turekian, K.K., 1985/86. The global-average production rate of ^{10}Be. Earth and Planetary Science Letters 76, 279-287.
Rudnick, R.L., Gao, S., 2004. Composition of the Continental Crust, in: Heinrich, D.H., Karl, K.T. (Eds.), Treatise on Geochemistry. Elsevier, Amsterdam, pp. 1-64.
Stallard, R.F., Edmond, J.M., 1987. Geochemistry of the Amazon weathering chemistry and limits to dissolved inputs. Journal of Geophysical Research 92, 8293-8302.
Staudigel, H., Albarède, F., Blichert-Toft, J., Edmond, J., McDonough, B., Jacobsen, S.B., Keeling, R., Langmuir, C.H., Nielsen, R.L., Plank, T., Rudnick, R., Shaw, H.F., Shirey, S., Veizer, J., White, W., 1998. Geochemical Earth Reference Model (GERM): description of the initiative. Chemical Geology 145, 153-159.
Taylor, A., Blake, W.H., Couldrick, L., Keith-Roach, M.J., 2012. Sorption behaviour of beryllium-7 and implications for its use as a sediment tracer. Geoderma 187-188, 16-23.
Viers, J., Roddaz, M., Filizola, N., Guyot, J.-L., Sondag, F., Brunet, P., Zouiten, C., Boucayrand, C., Martin, F., Boaventura, G.R., 2008. Seasonal and provenance controls on Nd-Sr isotopic compositions of Amazon rivers suspended sediments and implications for Nd and Sr fluxes exported to the Atlantic Ocean. Earth and Planetary Science Letters 274, 511-523.
von Blanckenburg, F., O'Nions, R.K., 1999. Response of beryllium and radiogenic isotope ratios in Northern Atlantic Deep Water to the onset of Northern Hemisphere Glaciation. Earth and Planetary Science Letters 167, 175-182.
von Blanckenburg, F., O'Nions, R.K., Belshaw, N.S., Gibb, A., Hein, J.R., 1996. Global distribution of Beryllium isotopes in deep ocean water as derived from Fe-Mn crusts. Earth and Planetary Science Letters 141, 213-226.
Vonmoos, M., Beer, J., Muscheler, R., 2006. Large variations in Holocene solar activity: constraints from ^{10}Be in the Greenland Ice Core Project ice core. Journal of Geophysical Research 111, doi.10.1029/2005JA011500.
Willenbring, J.K., von Blanckenburg, F., 2010a. Long-term stability of global erosion rates and weathering during late-Cenozoic cooling. Nature 465, 211-214.
Willenbring, J.K., von Blanckenburg, F., 2010b. Meteoric cosmogenic Beryllium-10 adsorbed to river sediment and soil: applications for Earth-surface dynamics. Earth Science Reviews 98, 105-122.
Wittmann, H., von Blanckenburg, F., Bouchez, J., Dannhaus, N., Naumann, R., Christl, M., Gaillardet, J., 2012. The dependence of meteoric ^{10}Be concentrations on particle size in Amazon River bed sediment and the extraction of reactive ^{10}Be/^{9}Be ratios. Chemical Geology 318-319, 126-138.
Wittmann, H., von Blanckenburg, F., Guyot, J.L., Laraque, A., Bernal, C., Kubik, P.W., 2010. Sediment production and transport from in situ-produced cosmogenic ^{10}Be and river loads in the Napo River basin, an upper Amazon tributary of Ecuador and Peru. Journal of South American Earth Sciences 31, 45-53.
Wittmann, H., von Blanckenburg, F., Guyot, J.L., Maurice, L., Kubik, P.W., 2009. From source to sink: Preserving the cosmogenic ^{10}Be-derived denudation rate signal of the Bolivian Andes in sediment of the Beni and Mamoré foreland basins. Earth and Planetary Science Letters 288, 463-474.
Wittmann, H., von Blanckenburg, F., Maurice, L., Guyot, J.L., Filizola, N., Kubik, P.W., 2011. Sediment production and delivery in the Amazon River basin quantified by in situ–produced cosmogenic nuclides and recent river loads. Geological Society of America Bulletin 123, 10.1130/B30317.30311.
You, C.-F., Lee, T., Li, Y.-H., 1989. The partition of Be between soil and water. Chemical Geology 77, 105-118.
You, C.F., Lee, T., Brown, L., Shen, J.J., Chen, J.C., 1988. ^{10}Be study of rapid erosion in Taiwan. Geochim. Cosmochim. Acta 52, 2687-2691.

Online Supplement to:
Earth surface erosion and weathering from the ^{10}Be (meteoric)/^{9}Be ratio

Friedhelm von Blanckenburg, Julien Bouchez, and Hella Wittmann

Earth and Planetary Science Letters 2012, doi j.epsl.2012.07.022

S.1 Deriving equation (10) of the main text

Eq. (7) of the main text can be solved for *E*:

$$E = \frac{D*\left[{}^{9}Be\right]_{parent} - \frac{Q}{K_d}*\left[{}^{9}Be\right]_{reac}}{\left[{}^{9}Be\right]_{min}+\left[{}^{9}Be\right]_{reac}} \quad \text{(S1)}$$

The denominator of eq. (8) of the main text can thus be written:

$$D*\left[{}^{9}Be\right]_{parent} - E*\left[{}^{9}Be\right]_{min} = D*\left[{}^{9}Be\right]_{parent}*\left(1-\frac{\left[{}^{9}Be\right]_{min}}{\left[{}^{9}Be\right]_{min}+\left[{}^{9}Be\right]_{reac}}\left(1-\frac{Q*\left[{}^{9}Be\right]_{reac}}{K_d*D*\left[{}^{9}Be\right]_{parent}}\right)\right) \quad \text{(S2)}$$

$$= D*\left[{}^{9}Be\right]_{parent}*\left(1-\left(\frac{\left[{}^{9}Be\right]_{min}}{\left[{}^{9}Be\right]_{min}+\left[{}^{9}Be\right]_{reac}}-\frac{\left[{}^{9}Be\right]_{reac}}{\left[{}^{9}Be\right]_{min}+\left[{}^{9}Be\right]_{reac}}\frac{Q*\left[{}^{9}Be\right]_{min}}{K_d*D*\left[{}^{9}Be\right]_{parent}}\right)\right) \quad \text{(S3)}$$

$$= D*\left[{}^{9}Be\right]_{parent}*\left(\frac{\left[{}^{9}Be\right]_{reac}}{\left[{}^{9}Be\right]_{min}+\left[{}^{9}Be\right]_{reac}}\left(1+\frac{Q*\left[{}^{9}Be\right]_{min}}{K_d*D*\left[{}^{9}Be\right]_{parent}}\right)\right) \quad \text{(S4)}$$

And substituting eq. (S4) into eq. (8):

$$\left(\frac{^{10}Be}{^{9}Be}\right)_{reac} = \left(\frac{^{10}Be}{^{9}Be}\right)_{diss} = \frac{\frac{^{10}Be}{F_{met}}\left(\frac{\left[{}^{9}Be\right]_{min}}{\left[{}^{9}Be\right]_{reac}}+1\right)}{1+\frac{Q}{K_d}*\frac{\left[{}^{9}Be\right]_{min}}{D*\left[{}^{9}Be\right]_{parent}}} \quad \text{(S5)}$$

S.2 The apparent Q/K_d-dependence of eqs. (10) and (11) in the main text

Intuitively, the isotope ratio ($^{10}Be/^{9}Be)_{reac}$ or ($^{10}Be/^{9}Be)_{diss}$ should neither depend on *Q* (water flux) nor on K_d (partition coefficient of Be between the dissolved and the reactive phases), since both isotopes are affected in the same manner by water transport and incorporation into the reactive phase. It might therefore seem surprising that these ratios appear to depend on a $\frac{Q}{K_d}$ term in eq. (10) and (11) of the main text. This dependence is only an apparent one that is required for using eqs. (10) and (11). We can show that in reality neither *Q* nor K_d control ($^{10}Be/^{9}Be)_{reac}$ or ($^{10}Be/^{9}Be)_{diss}$ since the numerator term of eqs. (10) and (11) ($[^{9}Be]_{min}/[^{9}Be]_{reac}$+1) is also dependent on $\frac{Q}{K_d}$ *via* eq. (5) of the main text:

$$\frac{[\,^9Be]_{min}}{[\,^9Be]_{reac}} + 1 = \frac{D*[\,^9Be]_{parent} - Q*[\,^9Be]_{diss}}{E*[\,^9Be]_{reac}} = \frac{D}{E} * \frac{[\,^9Be]_{parent}}{[\,^9Be]_{reac}} - \frac{Q}{K_d} \qquad \text{(S6)}$$

The dependence on $\frac{Q}{K_d}$ in eqs. (10) and (11) actually cancels out, as can be shown algebraically by rearranging eqs. (10) and (11) using eq. (S6).

S.3 Modelling the effect of sediment storage on $(^{10}Be/^{9}Be)_{reac}$ in Amazon river sediment

The Amazon data shown in Figure 6 of the main text shows that for rivers draining the Brazilian Shield, modeled $f_{reac}^{\ ^9Be} + f_{diss}^{\ ^9Be}$ is too low for the weathering regime encountered there. Provided that our assumptions on $[^9Be]_{parent}$ and ^{10}Be flux are valid for the Brazilian Shield, and the denudation rates from *in situ*-produced ^{10}Be are accurate, a possible explanation is that these samples have been affected by sediment storage in floodplains. Storage exceeding >10^5 years in duration can lead to both the radioactive decay of ^{10}Be in deeply stored sediment, or to its increase by exposure to meteoric flux in shallow sedimentary deposits. Tapping of old deposits by river avulsions leads to the entrainment of coarse quartz grains into the rivers draining the cratonic Brazilian and Guayana shield (Wittmann et al., 2011b). These coarse quartz grains yield *in situ* ^{26}Al/^{10}Be ratios that indicate storage by up to 1 My (Wittmann et al., 2011b). This sediment is then mixed with modern sediment in the river.

In Figure S1 we model the effect on $(^{10}Be/^{9}Be)_{reac}$ by ^{10}Be accumulation and –decay in such stored sediment by calculating the inventory in a vertical column of floodplain sediment following equation (6) of Willenbring and von Blanckenburg (2010), and using a long-term storage model similar to that of Wittmann and von Blanckenburg (2009). We use sediment storage depths of 10 m and 50 m respectively, a constant $[^9Be]_{reac}$ during storage of 0.5 ppm, two initial $[^{10}Be]_{reac}$ values corresponding to denudation rates prevailing in the sediment´s source areas of 20 (case a in Figure S1) and 300 t km^{-2} yr^{-1} (case b in Figure S1), respectively, and a decay constant for ^{10}Be of 5 × 10^{-7} yr^{-1}. We assume that the stored sediment receives additional meteoric ^{10}Be from precipitation with a flux typical for the Amazon basin of 0.8× 10^6 atoms cm^{-2} yr^{-1} (Willenbring and von Blanckenburg 2010), which is quantitatively retained and is then mixed and homogenised (through bank erosion, for example) with the initial $[^{10}Be]_{reac}$ and the initial $[^9Be]_{reac}$. Results (scale bars in Fig. S1 represent storage durations of 0.5, 1, 2, and 3 My) show that for the low initial $[^{10}Be]_{reac}$ case b, $(^{10}Be/^{9}Be)_{reac}$ increases, and the extent of increase depends on storage depth. For the high initial $[^{10}Be]_{reac}$ case a, 10 m deep sediment storage case results in an increase too, while in the 50 m case the initial $[^{10}Be]_{reac}$ decays radioactively.

Hence, the minor increased $(^{10}Be/^{9}Be)_{reac}$ of Brazilian Shield values (between 0.15 and 0.6) over a ratio expected from weathering kinetics (with a $f_{reac}^{\ ^9Be} + f_{diss}^{\ ^9Be}$ value probably close to 1 which is similar to Guyana Shield values) can potentially be explained by shallow intermittent storage. For all non-Brazilian Shield samples, we see no evidence for being biased by containing previously stored sediment. Indeed, in the

Amazon trunk stream, the sediment is derived from Andean sources, and $^{26}Al/^{10}Be$ ratios indicate no signs of burial (Wittmann et al., 2011b).

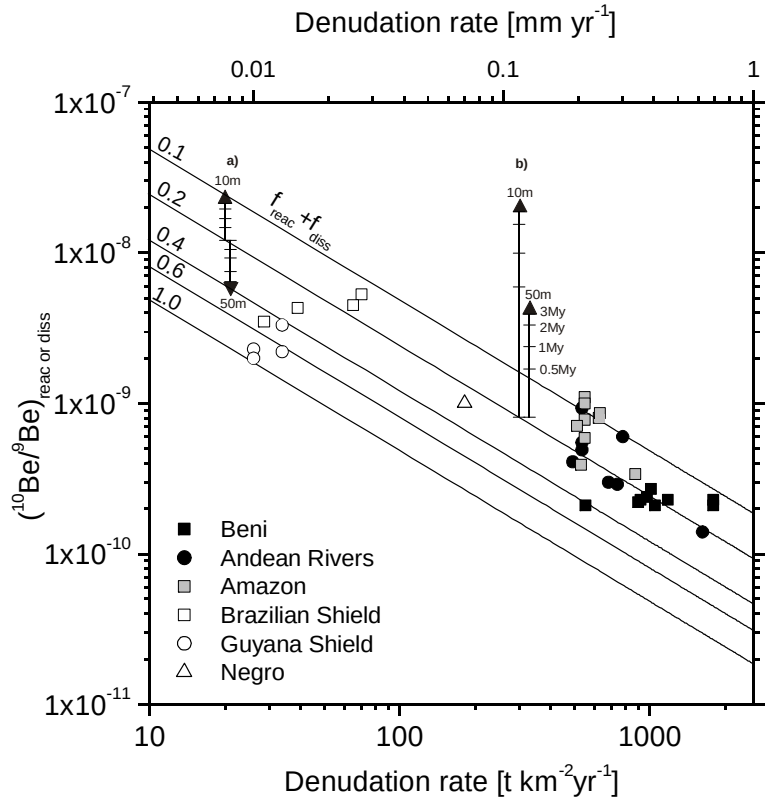

Figure S1: The potential effect of sediment storage in large basins on the $(^{10}Be/^{9}Be)_{reac}$ ratio. The data shown is the same as in Figure 6 of the main text. In addition, potential changes in $(^{10}Be/^{9}Be)_{reac}$ are shown by the scale bars for burial depths of 10 m and 50 m, respectively, by using initial, that is pre-burial $[^{10}Be]_{reac}$, which correspond to *D* of 20 (case a) and 300 t km^{-2} yr^{-1} (case b), respectively, measured in the sediment´s source area. We also assume an initial (pre-burial) and constant $[^{9}Be]_{reac}$ of 0.5 ppm. Tick marks for the duration of storage (shown only on the right-most scale bar, case b) are the same for all models. Note that in all cases burial leads to an increase in the $^{10}Be/^{9}Be$ ratio, unless the initial ^{10}Be concentration is high (meaning low *D*) and storage is deep where there is net decay of ^{10}Be (case a, 50 m storage depth).

Supplementary Table 1: New Amazon data							
			Lat/Long	**Grain size**	**(^{10}Be/^{9}Be)$_{reac}$**	**[^{9}Be]$_{reac}$**	**[^{9}Be]$_{min}$**
Sample	River	Setting	**(° UTM)**	**(µm)**		**(ppm)**	**(ppm)**
Be 1	Beni trunk	Boliv. Andes	-14.5273 / -67.4969	<30-125	2.44E-10	0.45	1.00
Be 2-1	Beni trunk	Boliv. Andes	-14.2844 / -67.4737	30-40	2.29E-10	0.41	0.95
Be 2-2	Beni trunk	Boliv. Andes	-14.2844 / -67.4737	30-40	2.10E-10	0.39	N.A.*
Be 3	Beni trunk	Boliv. Andes	-13.5713 / -67.3533	30-40	2.31E-10	0.37	N.A.
Be 4	Beni trunk	Boliv. Andes	-13.1191 / -67.1846	30-40	2.07E-10	0.43	N.A.
Be 8	Beni trunk	Boliv. Andes	-12.0777 / -66.8819	30-40	2.13E-10	0.31	N.A.
Be 10	Beni trunk	Boliv. Andes	-11.5585 / -66.6766	30-40	2.20E-10	0.35	1.15
Be 12	Beni trunk	Boliv. Andes	-11.2125 / -66.2488	30-40	2.29E-10	0.36	N.A.
Be 17	Beni trunk	Boliv. Andes	-10.5500 / -65.6000	30-40	2.73E-10	0.33	1.24
MD 15	Madre de Dios	Boliv. Andes	-11.1123 / -66.4159	30-40	2.88E-10	0.40	1.05
GR 19	Grande	Bolivian Andes	-18.9091 / -63.4095	30-40	1.42E-10	0.52	0.91
Mar 18	Mamoré	Boliv. Andes & Brazl. Shield	-10.8078 / -65.3458	30-40	4.12E-10	0.31	1.04
Mad 19	Upper Madeira	Boliv. Andes & Brazl. Shield	-10.2292 / -65.2811	30-40	3.01E-10	0.39	N.A.
Mad 20	Upper Madeira	Boliv. Andes & Brazl. Shield	-8.7703 / -63.9092	30-40	5.99E-10	0.30	1.02
Pe 101	Solimoes-Upper Amazon	Peruv./Ecuad. Andes	-3.5988 / -73.1373	30-40	3.85E-10	0.25	0.92
Pe 107	Ucayali	Peruv./Ecuad. Andes	-4.4794 / -73.4263	30-40	3.44E-10	0.20	N.A.
Man 2.4	Amazon at Manacapuru	Lowlands	-3.3202 / -60.5541	30-40	7.99E-10	0.24	N.A.
Ir 1.75	Amazon at Iracema	Lowlands	-3.3288 / -58.8287	30-40	8.62E-10	0.44	N.A.
Par 0.9	Amazon at Parintins	Lowlands	-3.4107 / -58.7793	30-40	1.07E-09	0.38	0.94
Par 1.2	Amazon at Parintins	Lowlands	-2.5831 / -56.6550	30-62	7.84E-10	0.27	N.A.
Par 1.6	Amazon at Parintins	Lowlands	-2.5755 / -56.6589	30-40	5.91E-10	0.26	0.92
Par 2.2	Amazon at Parintins	Lowlands	-2.5992 / -56.6667	30-40	1.04E-09	0.39	N.A.
Obi	Amazon at Óbidos	Lowlands	-1.9359 / -55.4989	<30-250	7.10E-10	0.28	0.69
Mad 0.3	Lower Madeira	Lowlands	-3.4055 / -58.7913	30-40	5.54E-10	0.65	1.33
Mad 0.5	Lower Madeira	Lowlands	-3.4044 / -58.7883	30-62	4.85E-10	0.33	1.52
Mad 1.8	Lower Madeira	Lowlands	-3.4107 / -58.7793	30-40	9.29E-10	1.14	N.A.
Cb 2	Guaporé	Brazilian Shield	-13.4829 / -61.0446	<30-125	5.26E-09	0.32	0.47
Cb 3	Aripuana	Brazilian Shield	-10.1696 /-59.4661	30-40	3.51E-09	0.84	0.92
Cb 5	Apiacás	Brazilian Shield	-9.9357 / -56.9372	30-62	4.30E-09	0.21	0.79
Cb 6	Teles Pires	Brazilian Shield	-9.6391 / -56.0191	30-62	4.45E-09	0.41	0.91
Br 2	Branco	Guyana Shield	1.8167 / -61.0422	90-125	2.33E-09	0.16	N.A.
Br 3	Branco	Guyana Shield	1.4099 / -61.2786	125-250	2.04E-09	0.07	0.13
Br 4	Branco	Guyana Shield	1.3015 / -61.2993	125-250	2.19E-09	0.10	N.A.

Br 7	Branco	Guyana Shield	-0.3425 / -61.8022	<30-125	3.28E-09	0.05	0.75
Ne 0.6	Negro	Guyana Shield	-3.0755 /-60.2261	125-250	1.04E-09	0.06	0.20

This table summarises data used for Fig. 6, Fig. 7, and Table 2 of the main text. N.A.: no data available. The original Be isotope data of most of these samples is published in Wittmann et al. (2012). The discharge data used to calculate fluxes in Table 2 of the main text are from the following sources: Amazon at Obidos (Filizola and Guyot, 2009); Solimoes at Manacapuru (Coe et al., 2002); Negro at Manaus (Moreira-Turcq et al., 2003); Andean Rivers (Madre de Dios, Grande, upper Soli, Ucayali) (Moquet et al., 2011); Beni (Guyot et al., 1993).

Supplementary Table 2a: Denudation Rates from $^{10}Be/^{9}Be$(diss) and yields from global rivers									
River	**Sample number**	**$(^{10}Be/^{9}Be)_{diss}$**	**$[^{9}Be]_{reac}$**	**F^{10Be}_{met}**	**$D(^{10}Be/^{9}Be)_{diss}$**	**Sediment yield**	**Dissolved yield**	**Total yield**	**Yield Data Source**
				atoms/km^2/yr	**t/km^2/yr**	**t/km^2/yr**	**t/km^2/yr**	**t/km^2/yr**	
W USA Rivers (Kusakabe et al. 1991)									
Columbia River	1	1.06E-08	9.89E-10	1.00E+16	28.5	10	31	41	M&F, 2011
Santa Ana River (I)	5	6.30E-09	2.91E-09	1.00E+16					
Santa Ana River (2)	6	7.60E-09	8.98E-10	1.00E+16					
Santa Ana River (3)	7	6.80E-09	1.15E-09	1.00E+16					
Santa Ana River (4)	8	7.20E-09	1.80E-09	1.00E+16					
Santa Ana River (5)	9	9.40E-07	1.19E-07	1.00E+16					
Santa Ana Average 1-4 (5 = anomalous)		6.98E-09		1.00E+16	43.3	30	4.8	34.8	M&F, 2011
Sacramento River	13					30	22	52	M&F, 2011
San Joaquin River	20	1.22E-08	6.48E-10	1.00E+16	24.8	0	15.7	15.7	M&F, 2011
Klamath River	21	1.19E-08	9.26E-10	1.00E+16	25.4	240	39	279	M&F, 2011
Arctic Rivers (Frank et al. 2008)									
Mackenzie (67°26,0'N, 133°45,0'W)		3.60E-09	5.00E-10	6.00E+15	50.4	60	36	96	M&F, 2011
Ob (66°31,0'N, 66°36,0'E)		9.30E-09	1.00E-09	8.00E+15	26.0	10	11	21	M&F, 2011
Yenisey (69°23,0'N, 86°09,0'E)		1.54E-08	1.70E-09	5.00E+15	9.8	0	16.5	16.5	M&F, 2011
Lena (66°46,0'N, 123°22,0'E)		6.20E-09	7.00E-10	5.00E+15	24.4	10	24	34	M&F, 2011
Orinoco & Amazon (Brown et al. 1992)									
Amazon at Macapa	AM89-1	1.50E-09	4.00E-10	8.00E+15	161.2	190	43	233	M&F, 2011
Negro at Manaus	AM89-2	2.31E-09	3.00E-10	8.00E+15	104.7	140	57	197	M&F, 2011
Solimoes at Manaus	AM89-3	8.20E-10	1.27E-10	8.00E+15	295.0	250	47	297	Wittmann et al., 2011a
Amazon Estuary	AM89-17	1.43E-09	2.06E-10	8.00E+15	169.1	190	43	233	M&F, 2011
Orinoco	826	7.60E-10	1.00E-10	8.00E+15	318.2				
Orinoco	827	9.02E-10	1.20E-10	8.00E+15	268.1				
Orinoco Average	Average	8.31E-10		8.00E+15	291.0	190	30	220	M&F, 2011

Supplementary Table 2b: Denudation Rates from $^{10}Be/^{9}Be$(reac) and *in situ*-produced ^{10}Be in the Amazon basin								
Sample	**Grain Size**	**$(^{10}Be/^{9}Be)_{reac}$**	**$[^{9}Be]_{reac}$**	**F^{10Be}_{met}**	**$D(^{10}Be/^{9}Be)_{reac}$**	**D (*in situ* ^{10}Be)**	**±**	**Total yield**
				atoms/km^2/yr	**t/km^2/yr**	**mm/yr**	**mm/yr**	**t/km^2/yr**
Be 1 AVG	<30-125	2.44E-10	2.0E-11	8.00E+15		0.375	0.063	975
Be 2-1Nad	30-40	2.29E-10	2.4E-11	8.00E+15		0.691	0.149	1798
Be 2-2HWO	30-40	2.10E-10	2.1E-11	8.00E+15		0.691	0.149	1798
Be 3	30-40	2.31E-10	2.0E-11	8.00E+15		0.454	0.057	1181
Be 4	30-40	2.07E-10	1.8E-11	8.00E+15		0.212	0.025	551
Be 8	30-40	2.13E-10	1.6E-11	8.00E+15		0.404	0.051	1051
Be 10	30-40	2.20E-10	2.0E-11	8.00E+15		0.345	0.032	896
Be 12	30-40	2.29E-10	3.9E-11	8.00E+15		0.353	0.084	918
Be 17	30-40	2.73E-10	2.5E-11	8.00E+15		0.389	0.069	1012
Average Beni					1049			1131
MD 15 Madre de Dios	30-40	2.88E-10	2.3E-11	8.00E+15	814	0.285	0.134	740
GR 19	30-40	1.42E-10	1.2E-11	8.00E+15	1706	0.625	0.090	1625
Mar 18 Mamoré	30-40	4.12E-10	3.3E-11	8.00E+15	570	0.189	0.058	492
Mad 19 upper Madeira	30-40	3.01E-10	2.3E-11	8.00E+15	803	0.263	0.038	685
Mad 20 upper Madeira	30-40	5.99E-10	4.5E-11	8.00E+15	392	0.300	0.035	780
Pe 101 Solimoes	30-40	3.85E-10	3.5E-11	8.00E+15	597	0.204	0.021	530
Pe 107 Ucayali	30-40	3.44E-10	3.2E-11	8.00E+15	702	0.337	0.036	877
Man 2.4 Manacapuru	30-40	7.99E-10	5.9E-11	8.00E+15	303	0.241	0.025	628
Ir 1.75 Iracema	30-40	8.62E-10	5.8E-11	8.00E+15	281	0.243	0.026	632
Par AVG Parintins	30-40	1.07E-09	6.6E-11	8.00E+15	284	0.211	0.022	549
OBI AVG Obidos	<30-250	7.10E-10	5.1E-11	8.00E+15	338	0.197	0.020	513
Mad AVG lower Madeira	30-40	5.54E-10	4.4E-11	8.00E+15	366	0.206	0.023	536
Cb 2 Guaporé, Brazl Shield AVG	<30-125	5.26E-09	3.8E-10	8.00E+15	41	0.027	0.003	71
Cb 3 Aripuana	30-40	3.51E-09	2.5E-10	8.00E+15	68	0.011	0.001	29
Cb 5 Apiacas	30-62	4.30E-09	3.0E-10	8.00E+15	58	0.015	0.001	39

Cb 6 Teles Pires	30-62	4.45E-09	3.1E-10	8.00E+15	54	0.025	0.002	65
Br 2 Branco, Guyana Shield	90-125	2.33E-09	1.6E-10	8.00E+15	104	0.010	0.001	27
Br 3	125-250	2.04E-09	1.5E-10	8.00E+15	119	0.010	0.001	27
Br 4	125-250	2.19E-09	1.4E-10	8.00E+15	110	0.013	0.001	34
Br 7	<30-125	3.28E-09	2.7E-10	8.00E+15	76	0.013	0.001	34
Ne 0.6 Negro, Guyana Shield	125-250	1.04E-09	8.3E-11	8.00E+15	232	0.070	0.006	182

Catchment-wide denudation rates *D* used in Figure 7 calculated from ^{10}Be/^{9}Be using eq. (9) for those global rivers for which an estimate of denudation rate with an independent method is available,. M&F, 2011: suspended and dissolved loads from Milliman and Farnsworth (2011). $(^{10}Be/^{9}Be)_{diss}$ data for North USA rivers is from Kusakabe et al. (1991); Arctic rivers are from Frank et al. (2008); South American rivers are from Brown et al. (1992). *D* from *in situ*-produced cosmogenic ^{10}Be measured in quartz on river bedload (Wittmann et al., 2011a) for the same samples on which $(^{10}Be/^{9}Be)_{reac}$ was determined (Wittmann et al., 2012). Uncertainty estimates in Figure 7 are ± 50% for *D* from river loads (taking into account an estimate for the differences that are commonly found when the decadal time scale estimates of suspended loads are compared with the millenial time scales for cosmogenic nuclides). Errors on *D* from *in situ*-produced ^{10}Be are the individual uncertainties that were reported for these estimates. Error on $D_{10Be/9Be}$ are estimated to be ± 50%, broadly combining uncertainties in estimates of $F_{met}^{^{10}Be}$ and $[^{9}Be]_{parent}$. Where multiple ^{10}Be/^{9}Be measurements are available for one river the resulting individual *D*'s were averaged. Only sample Santa Ana 5 (Kusakabe et al., 1991) was not used due to its unusual $(^{10}Be/^{9}Be)_{diss}$. $D_{10Be/9Be}$ was calculated using the individual basins $F_{met}^{^{10}Be}$ from Willenbring and von Blanckenburg (2010); $[^{9}Be]_{parent}$ of 2.5 ppm, and an $f_{reac}^{^{9}Be} + f_{diss}^{^{9}Be}$ of 0.2.

References cited in online supplement

Brown, E.T., Edmond, J.M., Raisbeck, G.M., Bourles, D., Yiou, F., Measures, C.I., 1992. Beryllium isotope geochemistry in tropical river basins. Geochim. Cosmochim. Acta 56, 1607-1624.

Coe, M.T., Costa, M.H., Botta, A., Birkett, C., 2002. Long-term simulations of discharge and floods in the Amazon Basin. Journal of Geophysical Research 107, 8044.

Filizola, N., Guyot, J., 2009. Suspended sediment yields in the Amazon basin: an assessment using the Brazilian national data set. Hydrological Processes 23, 3207-3215.

Frank, M., Backman, J., Jakobsson, M., Moran, K., O'Regan, M., King, J., A. Haley, B.A., Kubik, P.W., Garbe-Schönberg, D., 2008. Beryllium isotopes in central Arctic Ocean sediments over the past 12.3 million years: Stratigraphic and paleoclimatic implications. Paleoceanography 23, PA1S02, doi:10.1029/2007PA001478.

Guyot, J.L., Jouanneau, J.M., Quintanilla, J., Wasson, J.G., 1993. Dissolved and suspended sediment loads exported from the Andes by the Beni River (Bolivian Amazonia) during a flood. Geodinamica Acta 6, 233-241.

Kusakabe, M., Ku, T.L., Southon, J.R., Shao, L., Vogel, J.S., Nelson, D.E., Nakaya, S., Cusimano, G.L., 1991. Be isotopes in rivers/estuaries and their oceanic budgets. Earth and Planetary Science Letters 102, 265-276.

Milliman, J.D., Farnsworth, K.L., 2011. River discharge to the coastal ocean. A global synthesis. Cambridge University Press, Cambridge.

Moquet, J.S., Crave, A., Viers, J., Seyler, P., Armijos, E., Bourrel, L., Chavarri, E., Lagane, C., Laraque, A., Casimiro, W.S.L., Pombosa, R., Noriega, L., Vera, A., Guyot, J.L., 2011. Chemical weathering and atmospheric/soil CO_2 uptake in the Andean and Foreland Amazon basins. Chemical Geology 287, 1-26.

Moreira-Turcq, P., Seyler, P., Guyot, J.L., Etcheber, H., 2003. Exportation of organic carbon from the Amazon River and its main tribuatries. Hydrological Processes 17, 1329-1344.

Willenbring, J.K., von Blanckenburg, F., 2010. Meteoric cosmogenic Beryllium-10 adsorbed to river sediment and soil: applications for Earth-surface dynamics. Earth Science Reviews 98, 105-122.

Wittmann, H., von Blanckenburg, F., 2009. Cosmogenic nuclide budgeting of floodplain sediment transfer. Geomorphology 109, 246-256.

Wittmann, H., von Blanckenburg, F., Bouchez, J., Dannhaus, N., Naumann, R., Christl, M., Gaillardet, J., 2012. The dependence of meteoric ^{10}Be concentrations on particle size in Amazon River bed sediment and the extraction of reactive $^{10}Be/^{9}Be$ ratios. Chemical Geology 318-319, 126-138.

Wittmann, H., von Blanckenburg, F., Maurice, L., Guyot, J.L., Filizola, N., Kubik, P.W., 2011a. Sediment production and delivery in the Amazon River basin quantified by in situ–produced cosmogenic nuclides and recent river loads. Geological Society of America Bulletin 123, 10.1130/B30317.30311.

Wittmann, H., von Blanckenburg, F., Maurice, L., Guyot, J.L., Kubik, P.W., 2011b. Recycling of Amazon floodplain sediment quantified by cosmogenic Al-26 and Be-10. Geology 39, 467-470.